# Development of a portable gamma imaging system for absorbed radiation dose control in targeted radionuclide therapy

Carlotta TRIGILA
*PhD Student*

**Group IIRIC (Instrument. & Imagerie Radio-isotopique Clinique)**

**L. Ménard, P. Lanièce , Y. Charon, M.-A. Duval, M.-A.Verdier, L. Ammour, A. Bricou**

**Collaborations : AG medical, IRSN, European clinical centers (Londres, Utrecht)**

# Targeted internal radiotherapy

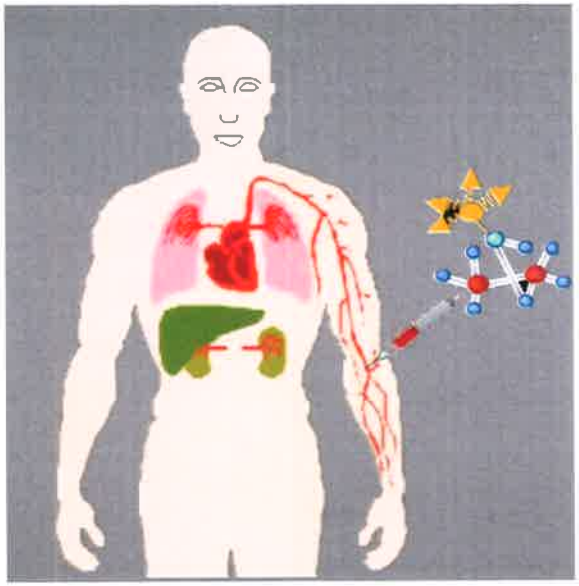

## Local irradiation with α or β emitting radionuclides

- $^{131}I$: Differentiated thyroid cancer and benign thyroid disease
- $^{131}I$-MIBG: Neuroendocrines tumors
- Palliative traitements due to osseous metastases : $^{32}P$, $^{89}Sr$, $^{153}Sm$-EDTMP, $^{186}Re/23^{8}Re$
- Rheumatologies : $^{90}Y$, $^{186}Re$, $^{169}Er$

- $^{90}Y$-ibritumomab tiuxetan (Zevalin) : lymphoma
- $^{90}Y$-microsphères: Liver tumor
- $^{223}Ra$ (Xofigo) : Prostate cancer with osseous metastases
- $^{90}Y/^{177}Lu$-DOTATOC/DOTATATE : Neuroendocrines tumors


**New radioisotopes / vector :**

**$^{149,161}Tb$, $^{225}Ac$,$^{211}At$,$^{212}Pb$,$^{227}Th$,$^{44}Sc$-$^{47}Sc$,$^{64}Cu$-$^{67}Cu$,$^{198-199}Au$**

# Targeted internal radiotherapy

## External Radiotherapy

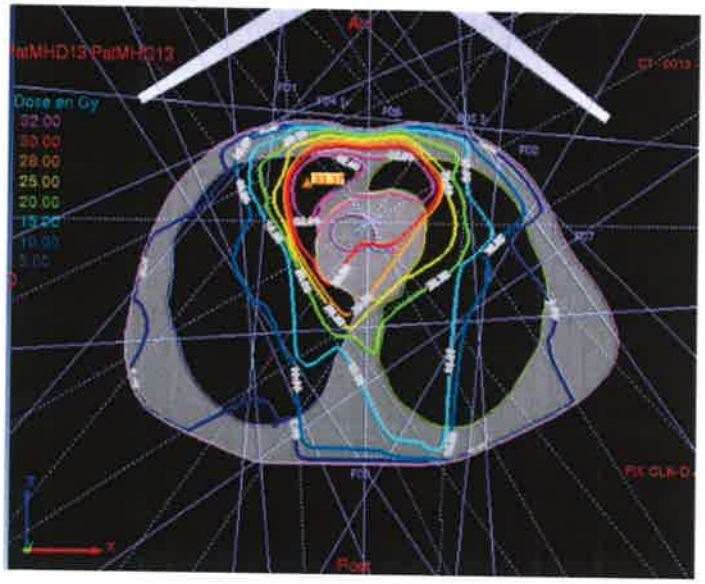

## Internal Radiotherapy


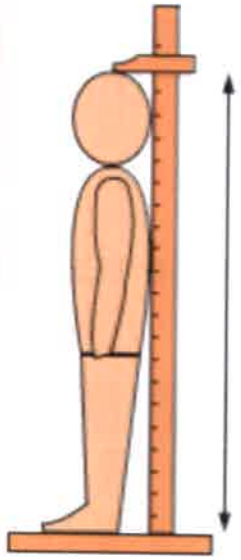

***height?***

***weight?***

## Observations :

**big differences in the observed effects (response and toxicity)**
**effects are dependent on the dose delivered to the tissues**

**Personalized dosimetry is essential for treatment's optimization (increase the dose in the tumor while sparing other organs)**

# Targeted internal radiotherapy

## External Radiotherapy

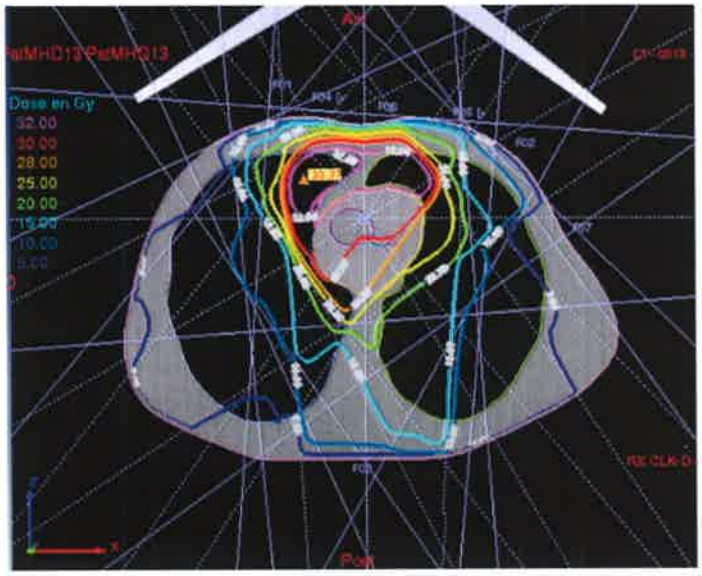


## Internal Radiotherapy


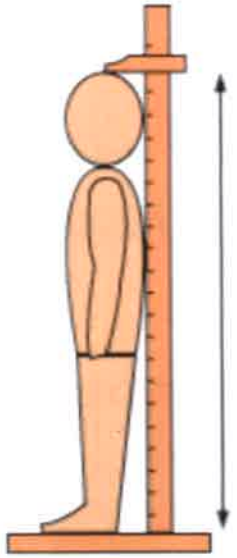

***height?***

***weight?***

## Decree-Law n° 2003-462 of 21 May 2003 on the regulatory disposition of parts I, II and III of the Public Health Code

### Article R. 1333-64

Pour les actes de médecine nucléaire à visée diagnostique, les médecins réalisateurs doivent mettre en oeuvre les moyens nécessaires pour maintenir la quantité de radioactivité des produits administrés **à la personne au niveau le** plus faible possible compatible avec l'obtention d'une information de qualité.

Pour les actes de médecine nucléaire à visée thérapeutique, les expositions des tissus et organes sont déterminées **au cas par cas,** en veillant à ce que les doses susceptibles d'être reçues par les organes et tissus autres que ceux directement visés par l'exposition soient maintenues au niveau le plus faible possible, compatible avec le but thérapeutique et la nature du ou des radionucléides utilisés.

# Imaging and Personalized Dosimetry

**Needs of a dosimetry based on quantitative imaging of the bio-distribution and kinetics of the radiopharmaceutical <u>for each patient</u> :**

1) Determine the activity to be injected

2) Determine the tolerance Dose

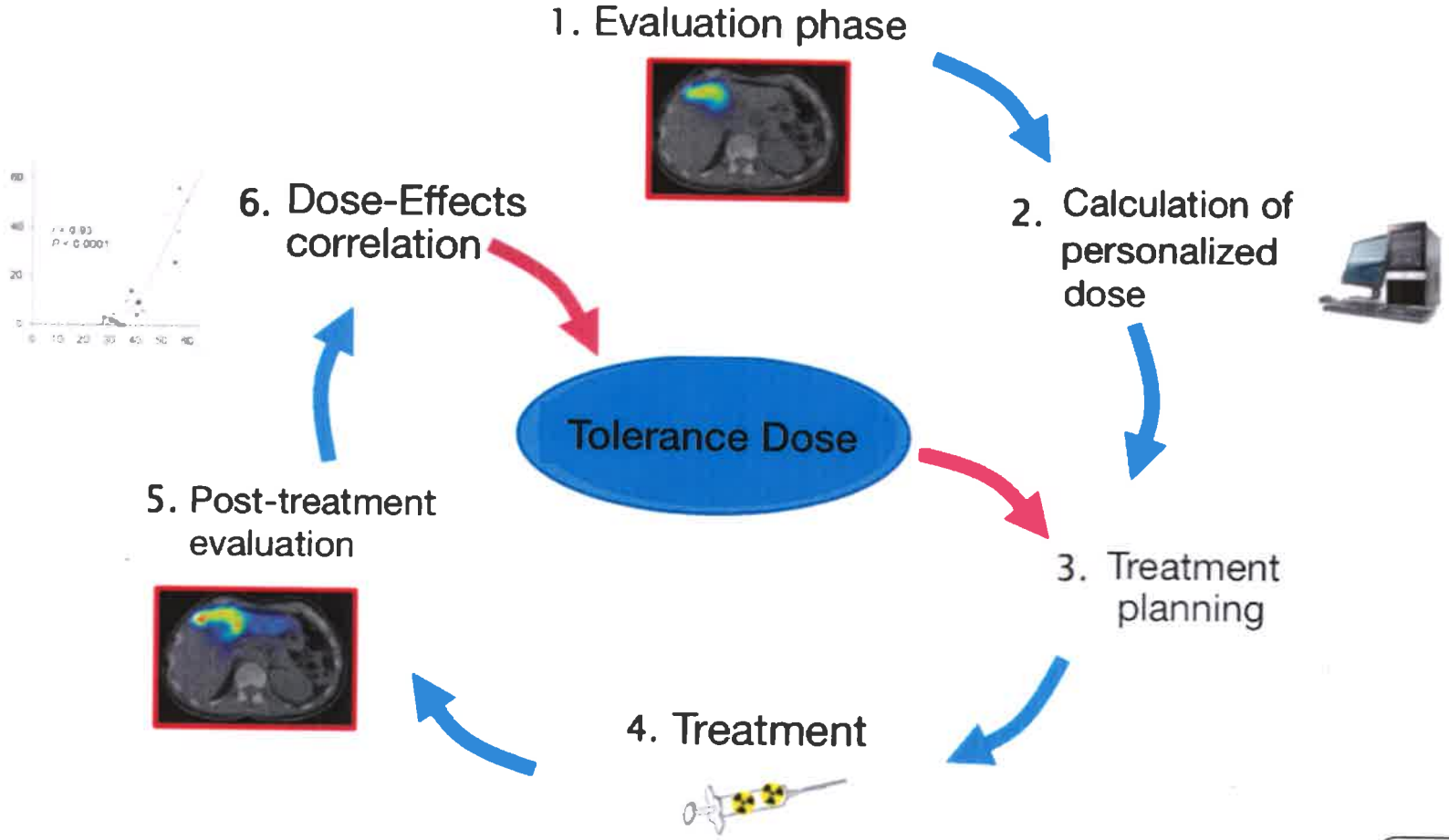

# Imaging and Personalized Dosimetry

## General interest of imaging just after patient injection :

**correlation between the dose released in the tumors/organs at risk and the clinical effect**

**verify that the uptake corresponds to the activity estimated from the evaluation phase**

**control the dose deposited during fractionated treatment, in order to eventually readjust it**

## Why lack of post-injection imaging nowadays ?

- the existing protocols are considered to be well working
- the new protocol is time consuming
- availability of the existing cameras for treatment imaging
- patient accessibility (radiation safety)
- cameras not optimized for all energies

## Why lack of post-injection imaging nowadays ?

- the existing protocols are considered to be well working
- the new protocol is time consuming
- availability of the existing cameras for treatment imaging
- patient accessibility (radiation safety)
- cameras not optimized for all energies

lack of specified detector

## Why lack of post-injection imaging nowadays ?

- the existing protocols are considered to be well working
- the new protocol is time consuming
- availability of the existing cameras for treatment imaging
- patient accessibility (radiation safety)
- cameras not optimized for all energies

lack of specified detector

**Development of mobile imaging systems for accurate measurements of absorbed doses delivered to the tumor and to the organs at risk just after the patient injection**

# Portable imaging systems for quantitative measurements of absorbed doses delivered to the patient during the treatment of thyroid disease (benign and malign)

# MoTI : Mobile Therapy Imager

## Portable imaging systems for quantitative measurements of absorbed doses delivered to the patient during the treatment of thyroid disease (benign and malign)

Treatments

- total/partial thyroidectomy
- high-dose radioactive $^{131}I$
- anti-thyroid drugs

# Portable imaging systems for quantitative measurements of absorbed doses delivered to the patient during the treatment of thyroid disease (benign and malign)

Treatments

total/partial thyroidectomy | high-dose radioactive $^{131}I$ | anti-thyroid drugs

## Hyperthyroidism

**Graves/Basedow disease**

hyperfunctioning and enlargement

380 ± 360 MBq

**Toxic nodular/ multinodular goiter**

*one or more* hyperfunctioning foci

640 ± 550 MBq

# MoTI : Mobile Therapy Imager

## Portable imaging systems for quantitative measurements of absorbed doses delivered to the patient during the treatment of thyroid disease (benign and malign)

Treatments

total/partial thyroidectomy | **high-dose radioactive $^{131}$I** | anti-thyroid drugs

### Hyperthyroidism

**Graves/Basedow disease**

hyperfunctioning and enlargement

380 ± 360 MBq

**Toxic nodular/ multinodular goiter**

*one or more* hyperfunctioning foci

640 ± 550 MBq

**High energy gamma rays (>300 keV)**

**High fluxes**

**Compact and mobile :**
Exams performed in an isolated room at the patient's bedside

**Spatial Resolution and Efficiency compromise**
for nodule detectability

**Good image contrast and signal to noise ratio**
for dose quantification

# MoTI : Mobile Therapy Imager

**Final purpose :**

## 10x10 $cm^2$ field of view miniaturized mobile gamma camera

- parallel-hole high-energy tungsten collimator
- continuous inorganic scintillator
- 256 channels photodetection system

# MoTI : Mobile Therapy Imager

**Final purpose :**

**10x10 cm$^2$ field of view miniaturized mobile gamma camera**

- parallel-hole high-energy tungsten collimator
- continuous inorganic scintillator
- 256 channels photodetection system

**Definition and optimization of the detection head (scintillator and collimator) of a first 5 x 5 cm$^2$ prototype in terms of spatial and energy resolution, efficiency and cost.**

**Experimental studies**

- Characterization of different inorganic scintillators/ photodetector assemblies

**Theoretical studies**

- Design of the collimator with analytical models and Monte Carlo simulation (*GATE*)
- Optimization of the overall camera with numerical phantoms

# Experimental studies

## Scintillators-photodetector characterization

- Crystals tested :
  $CeBr_3$ , $LaBr_3(Ce)$ , LYSO, LFS , GaGG
- Thickness : 6 mm and 1 cm
- Different optical coatings : diffusive, reflective, absorbing

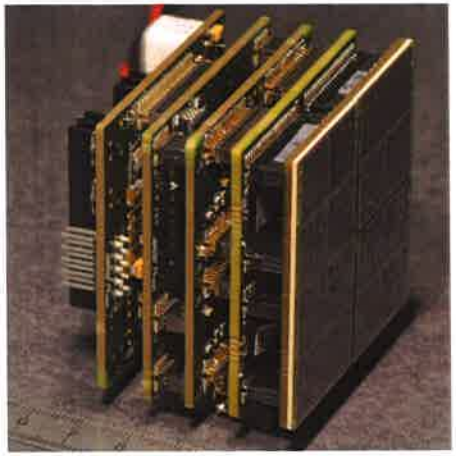

Photodetection system

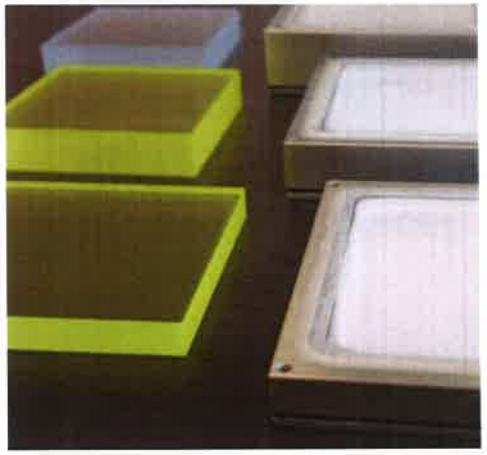

Incapsulated crystals

## Spectrometric Properties

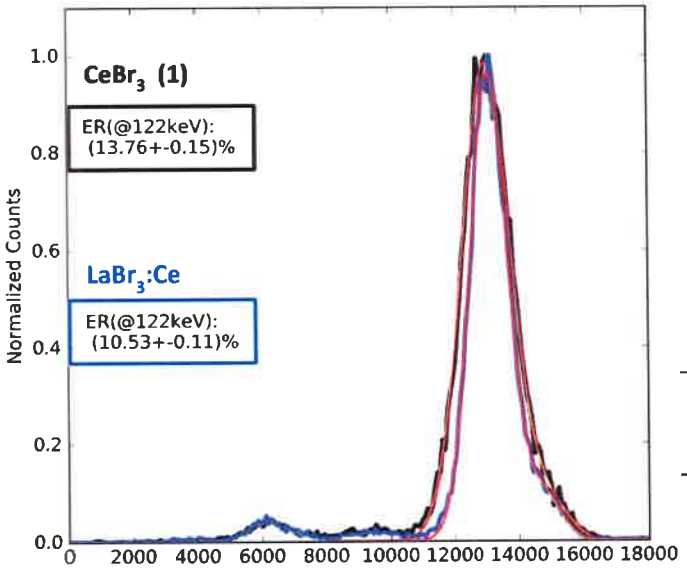


$CeBr_3$ 51 x 51 x 6 $mm_2$ (Absorbing edges) and $LaBr_3$ 51 x 51 x 6 $mm^2$

## Spatial Response

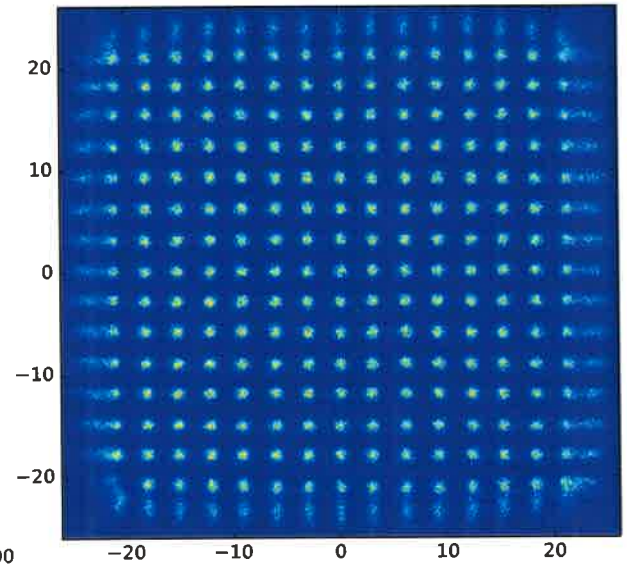


CeBr3 51 x 51 x 6 $mm^2$
Absorbing edges

## Results @ 122 keV

| | $LaBr_3$:Ce | $CeBr_3$ (1) | $CeBr_3$ (2) |
|---|---|---|---|
| Dimensions ($mm^3$) | 51x51x6 | 51x51x6 | 51x51x6 |
| Optical Coating | Abs | Abs | Refl |
| Light Guide (mm) | 1 | 1.5 | 2 |
| ΔE/E (%) @122 keV | 10.68 ± 0.81 | 13.81 ± 0.30 | 12.40 ± 0.20 |
| SR @ 122 keV (mm) | 1.00 ± 0.03 | 1.12 ± 0.03 | 1.34 ± 0.06 |
| Bias (mm) | 0.11 ± 0.09 | 0.13 ± 0.06 | 0.20 ± 0.08 |

# Monte Carlo simulations : What is GATE ?

**GATE: Opensource toolkit dedicated to the simulation of imaging (SPECT, PET, CT, Optical) and radiotherapy**

Broad range of applications:

- Detector design
- Optimization of acquisition and processing protocols
- Assessment of quantification methods
- Estimation of the system matrix used in tomographic reconstruction
- Dosimetry …

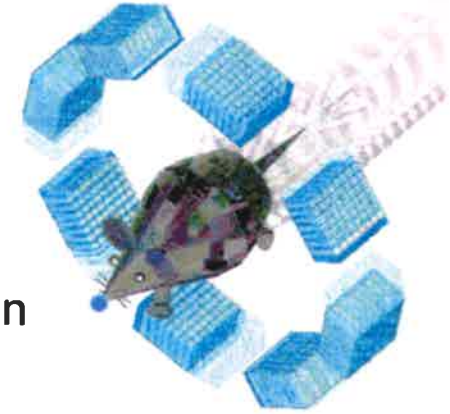

**19 labs, sharing developments and validation studies**

### France

- U892 Inserm, Nantes
- U1101 Inserm, Brest
- IMNC CNRS, Orsay
- LPC CNRS, Clermont Ferrand
- IPHC CNRS, Strasbourg
- UMR5515 CNRS, CREATIS, Lyon
- CPPM CNRS, Marseille
- Subatech CNRS, Nantes
- SHFJ CEA, Orsay
- U1037 Inserm, Toulouse

### Europe

- Delft University of Technology, Delft, The Netherlands
- Forschungszentrum Juelich, Germany
- National Technical University of Athens, Greece
- Medical University Vienna, Wien, Austria
- MedAustron. Wiener Neustadt. Wien. Austria

### Rest of the world

- Memorial Sloan-Kettering Cancer Center, New York, USA
- UC Davis, Davis, USA
- University of Santiago of Chile, Chile
- Sungkyunkwan University School of Medicine, Seoul, South Korea

# Monte Carlo simulations : What is GATE ?

## GATE: Opensource toolkit dedicated to the simulation of imaging (SPECT, PET, CT, Optical) and radiotherapy

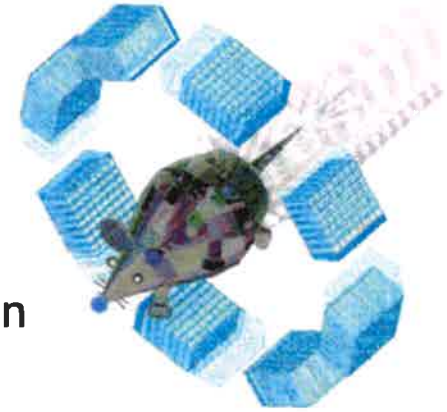

Broad range of applications:

- Detector design
- Optimization of acquisition and processing protocols
- Assessment of quantification methods
- Estimation of the system matrix used in tomographic reconstruction
- Dosimetry …

## GATE today : practical features

- Based on GEANT 4
- Written in C++
- Can be run on many platforms (Linux, Unix, MacOs)
- User-friendly: simulations can be designed and controlled using macros
- Flexible enough to model almost any detector design, including prototypes
- Explicit modeling of time (hence detector motion, patient motion, radioactive decay, dead time, time of flight, tracer kinetics)
- Can handle voxelized and analytical phantoms

# Theoretical studies : Collimator optimization

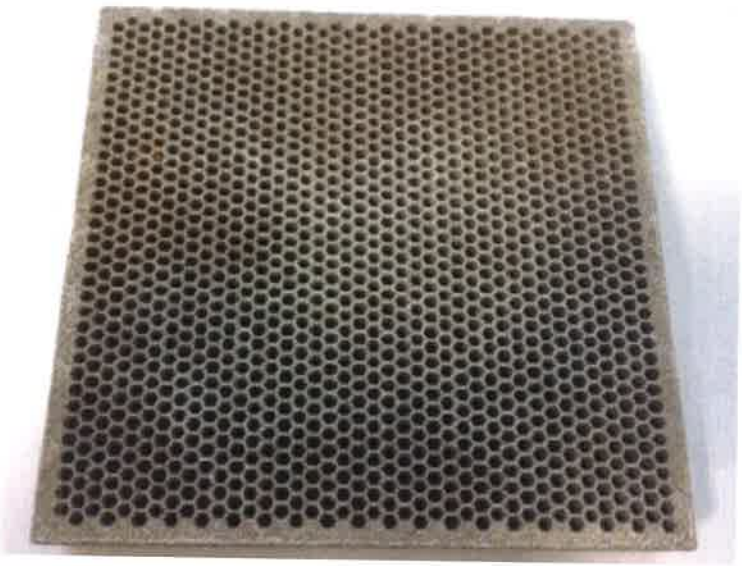

**Hexagonal parallel-hole high-energy tungsten collimator**

↓

**existing analytical model not suited for high energy gamma rays modeling**

# Theoretical studies : Collimator optimization

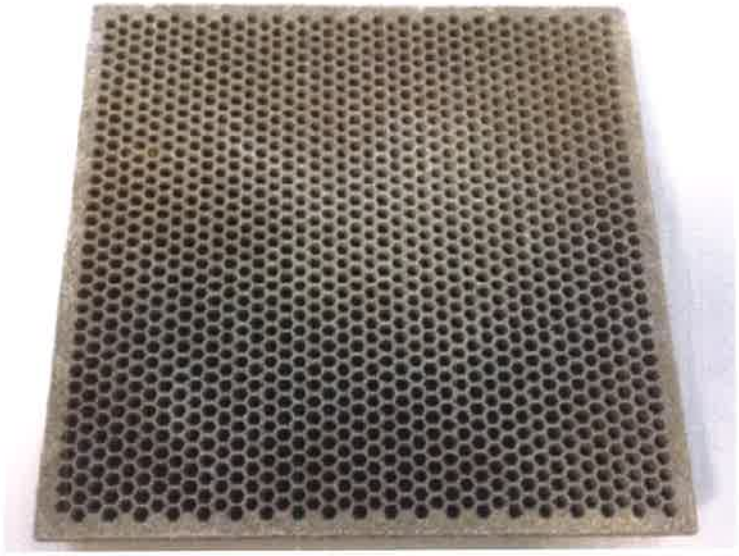

**Hexagonal parallel-hole high-energy tungsten collimator**

**existing analytical model not suited for high energy gamma rays modeling**

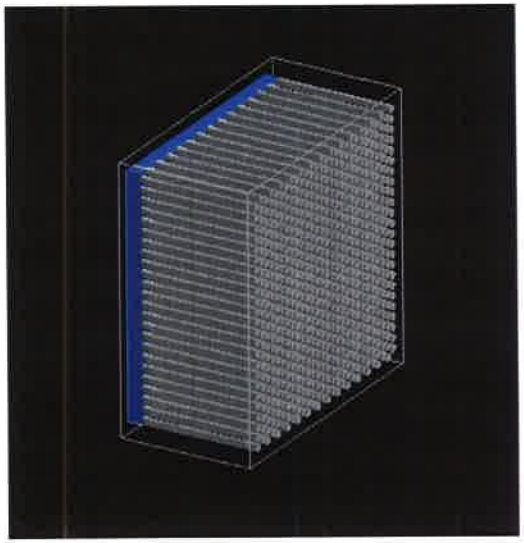

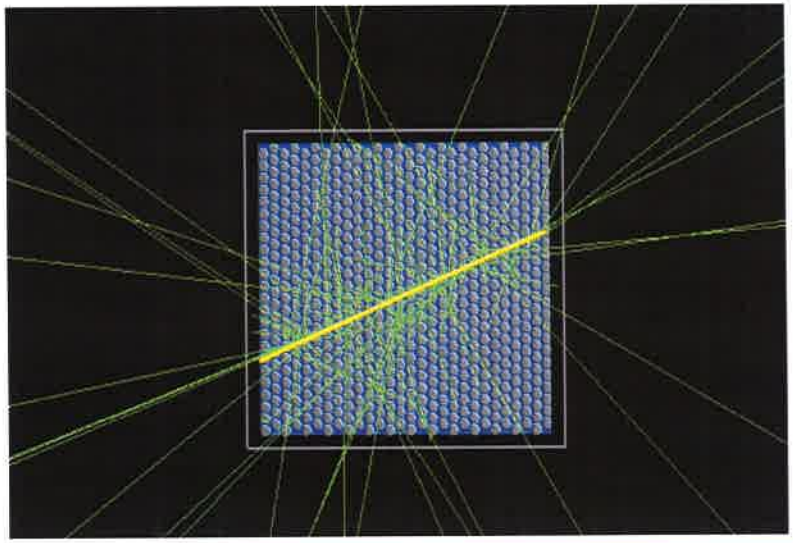

- **10x10 cm² FoV camera**
- **$^{131}$I line source in air**

| Gamma Emissions $^{131}$ I | | | | | |
|---|---|---|---|---|---|
| Energy (KeV) | 80,2 | 284,3 | 364,5 | 637 | 722,9 |
| BR % | 2,6 | 6,2 | 81,6 | 7,1 | 1,8 |

- **Collimator-to-source distance = 5 cm**

# Theoretical studies : Collimator optimization

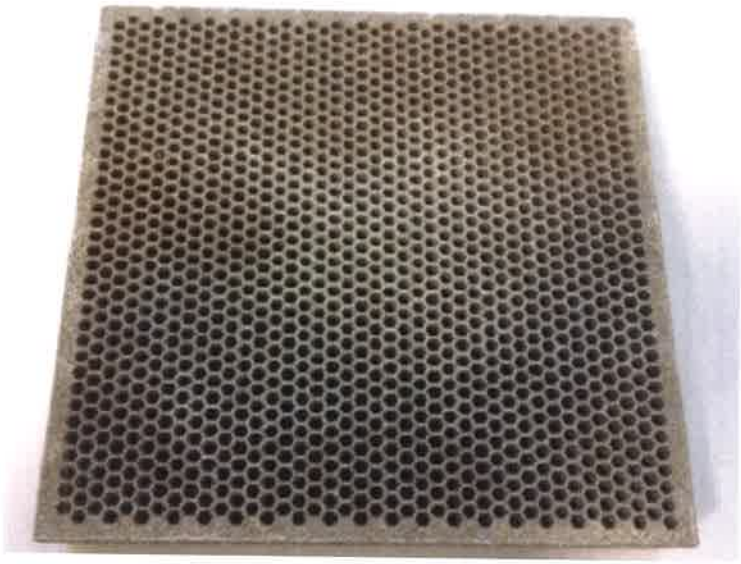

**Hexagonal parallel-hole high-energy tungsten collimator**

**existing analytical model not suited for high energy gamma rays modeling**

**SENSITIVE SURFACES**

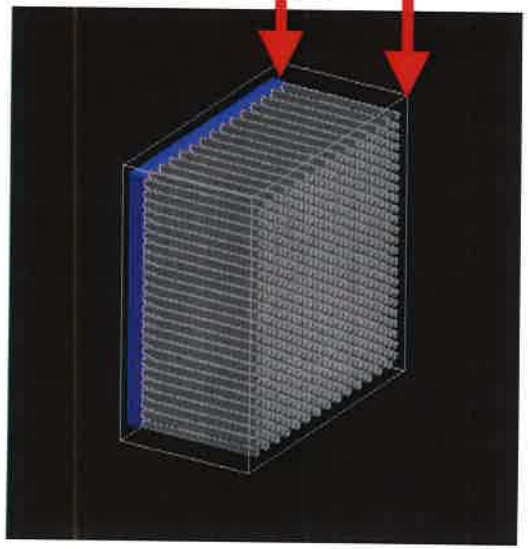

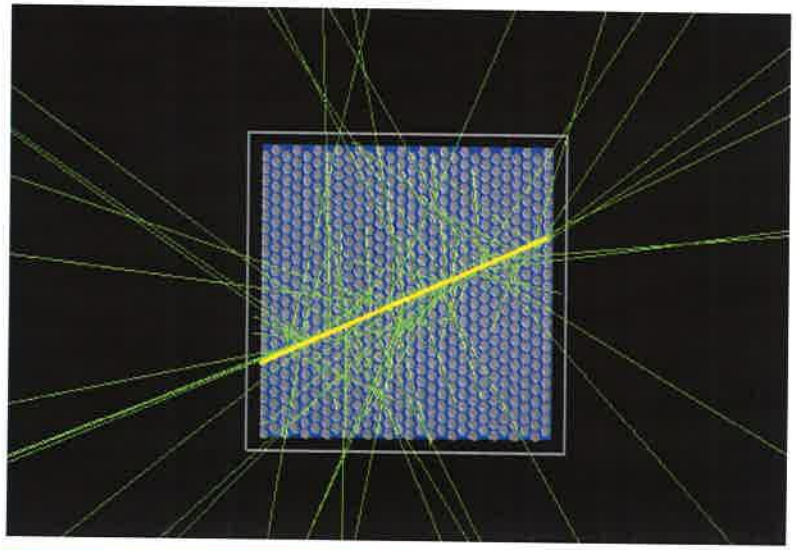

- **10x10 cm² FoV camera**
- **$^{131}$I line source in air**

| Gamma Emissions $^{131}$I | | | | | |
|---|---|---|---|---|---|
| Energy (KeV) | 80,2 | 284,3 | 364,5 | 637 | 722,9 |
| BR % | 2,6 | 6,2 | 81,6 | 7,1 | 1,8 |

- **Collimator-to-source distance = 5 cm**

# Collimator intrinsic properties : Insight

L Thickness

d Diameter

t Septa

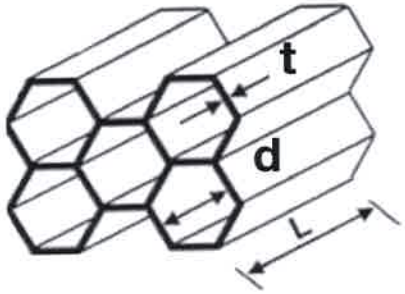


Simulated configurations :

- **L** ∈ [3,6.5] cm each 0.5 cm
- **d** ∈ [0.5,2.25] mm each 0.25 mm
- **t** ∈ [0.75,2.125] mm each 0.125 mm

# Collimator intrinsic properties : Insight

L Thickness

d Diameter

t Septa

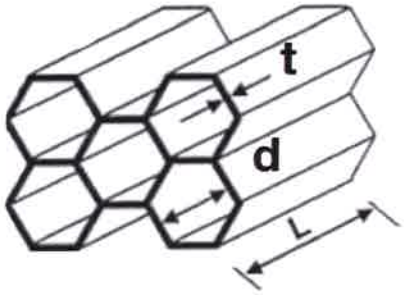


Simulated configurations :

- **L** ∈ [3,6.5] cm each 0.5 cm
- **d** ∈ [0.5,2.25] mm each 0.25 mm
- **t** ∈ [0.75,2.125] mm each 0.125 mm

## (1) Geometric Events

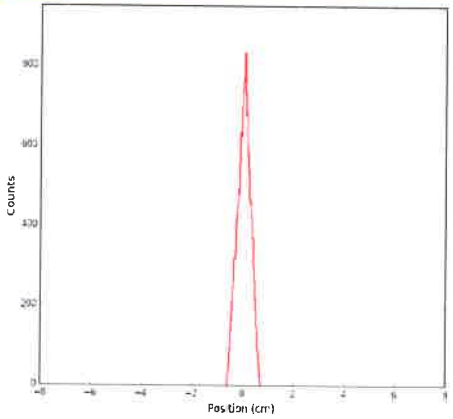


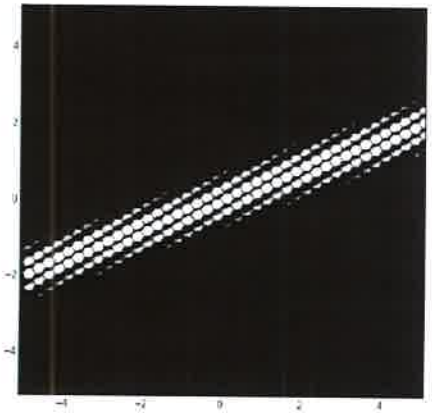

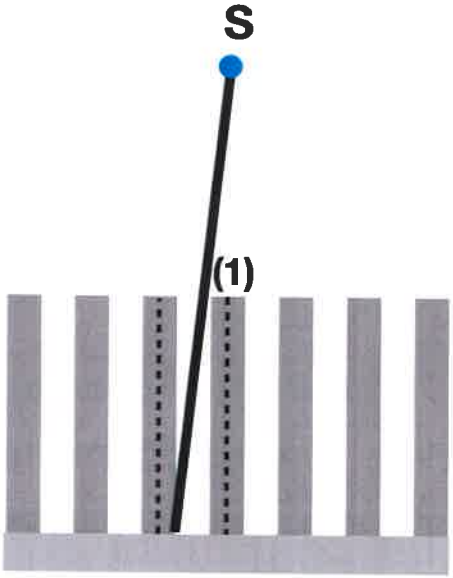

# Collimator intrinsic properties : Insight

**L Thickness**

**d Diameter**

**t Septa**

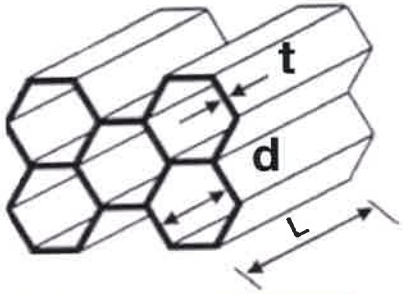


Simulated configurations :

- **L** ∈ [3,6.5] cm each 0.5 cm
- **d** ∈ [0.5,2.25] mm each 0.25 mm
- **t** ∈ [0.75,2.125] mm each 0.125 mm

**(1) Geometric Events**

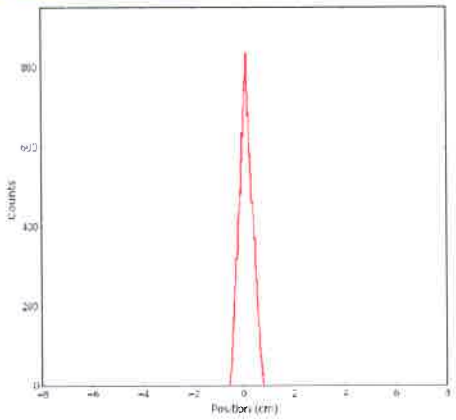


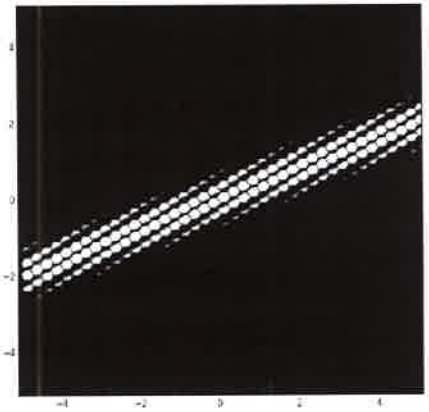

**(2) Penetration Events**

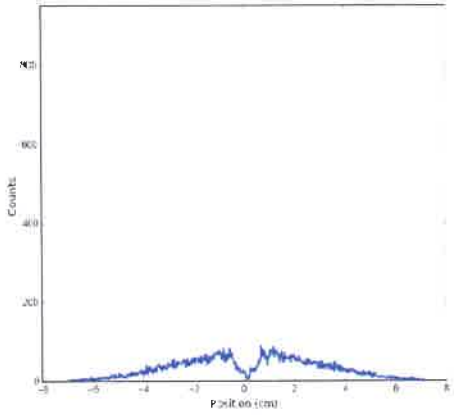


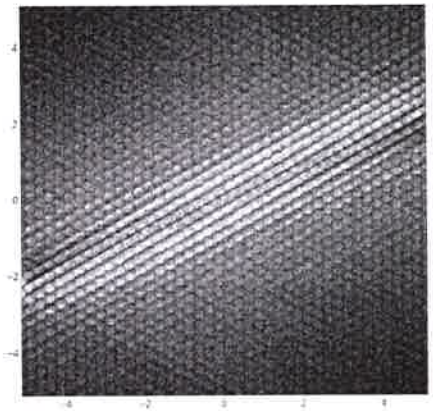

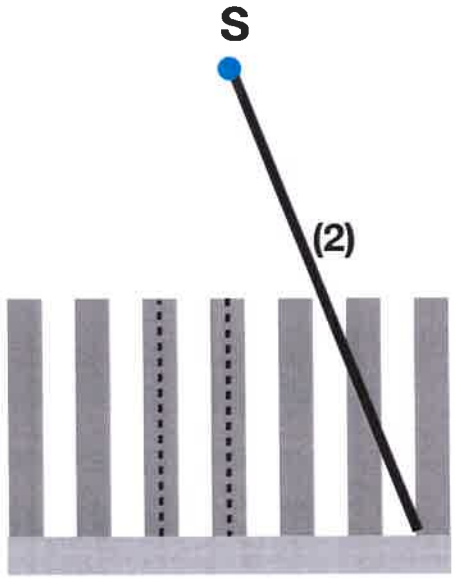

# Collimator intrinsic properties : Insight

L Thickness

d Diameter

t Septa

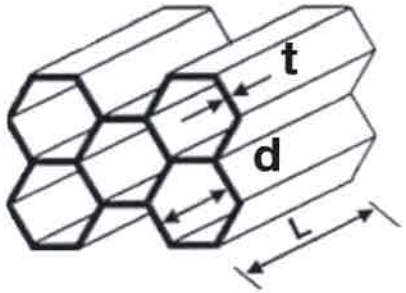


Simulated configurations :

- **L** ∈ [3,6.5] cm each 0.5 cm
- **d** ∈ [0.5,2.25] mm each 0.25 mm
- **t** ∈ [0.75,2.125] mm each 0.125 mm

## (1) Geometric Events

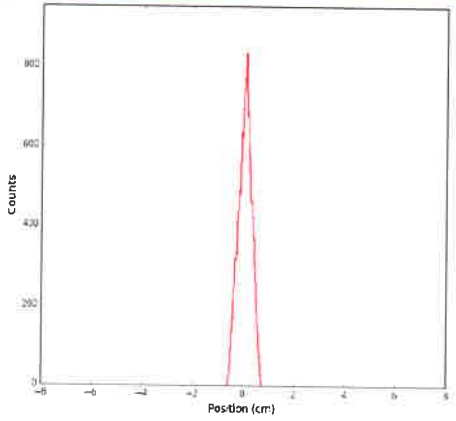


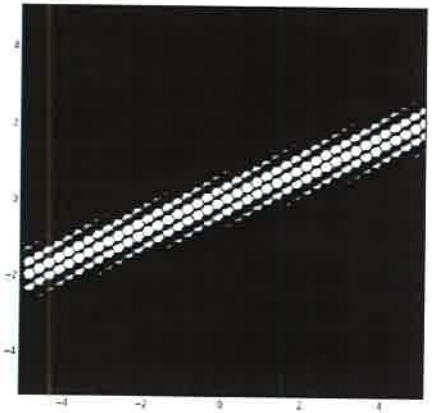

## (2) Penetration Events

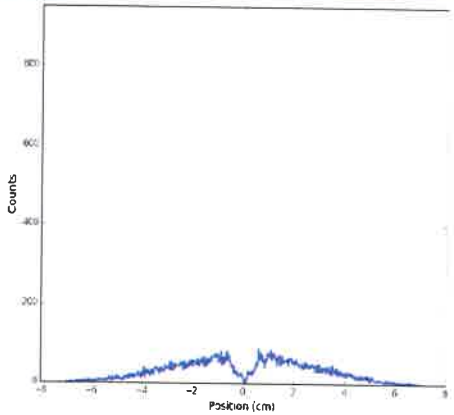


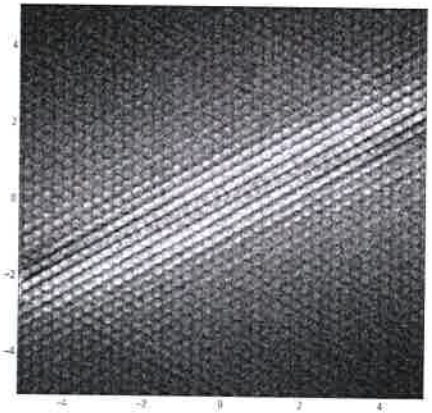

## (3) Scattered Events

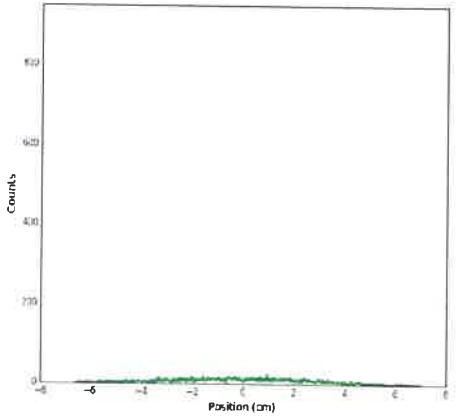


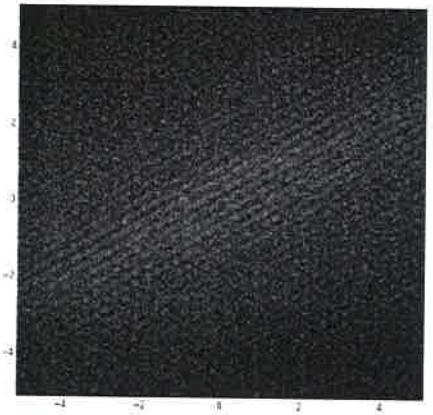

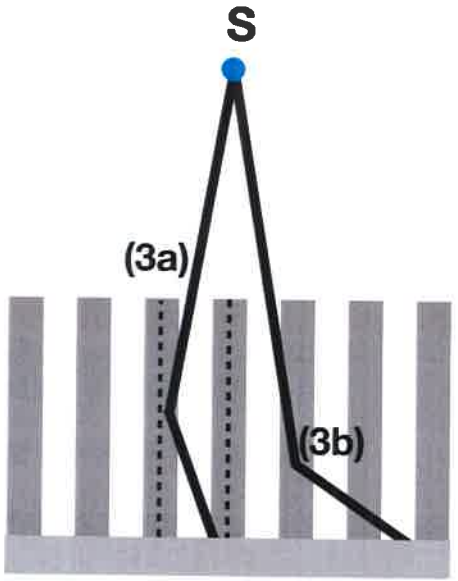

# Collimator intrinsic properties : Insight

L Thickness

d Diameter

t Septa

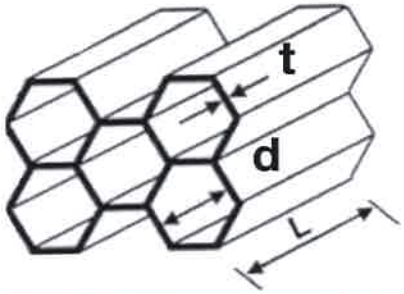


Simulated configurations :

- **L** ∈ [3,6.5] cm each 0.5 cm
- **d** ∈ [0.5,2.25] mm each 0.25 mm
- **t** ∈ [0.75,2.125] mm each 0.125 mm

| (1) Geometric Events | (2) Penetration Events | (3) Scattered Events | TOTAL Events |
|---|---|---|---|

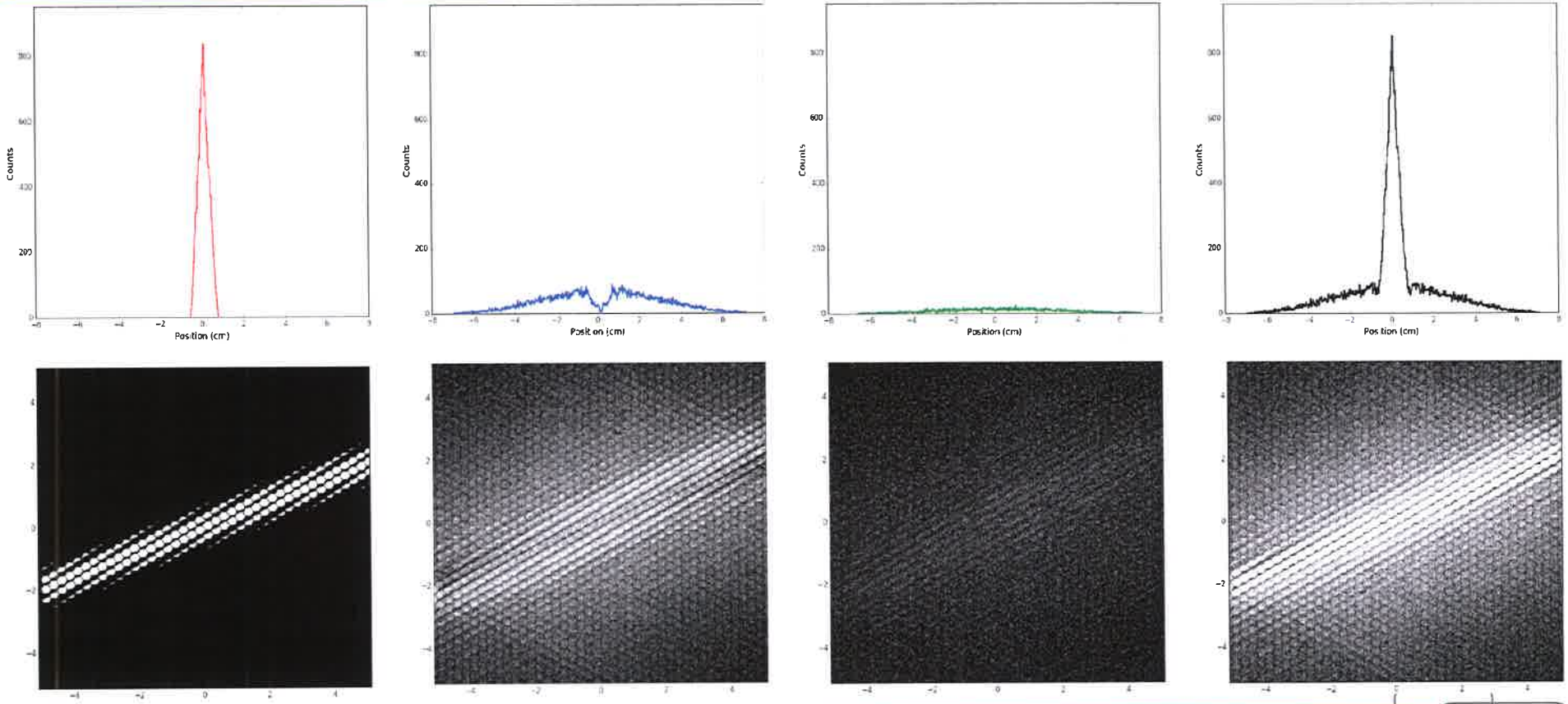

# Collimator intrinsic properties : Insight

*Septal Penetration* (**SP**)

*Efficiency* (**E**)

Spatial *Resolution* (**SR**)

# Collimator intrinsic properties : Insight

*Septal Penetration* (**SP**) | *Efficiency* (**E**) | Spatial *Resolution* (**SR**)

**Events (2+3b)**

**Detected Events**

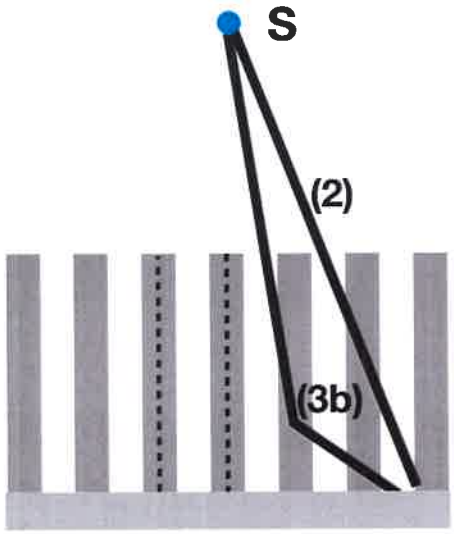


**(2) Penetration Events**

# Collimator intrinsic properties : Insight

**Septal Penetration (SP)**

**Events (2+3b) / Detected Events**

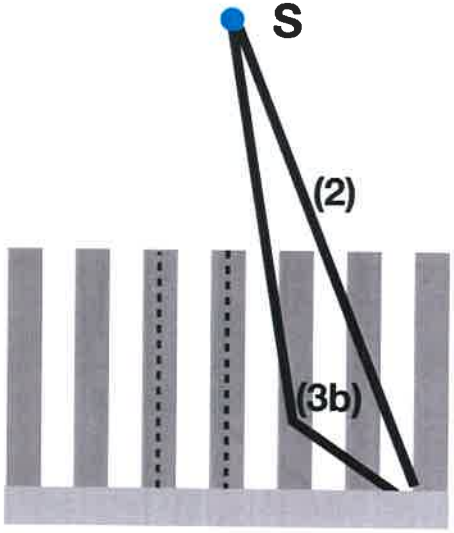


**(2) Penetration Events**

**Efficiency (E)**

**Total Events (1+2+3) / Emitted Activity**

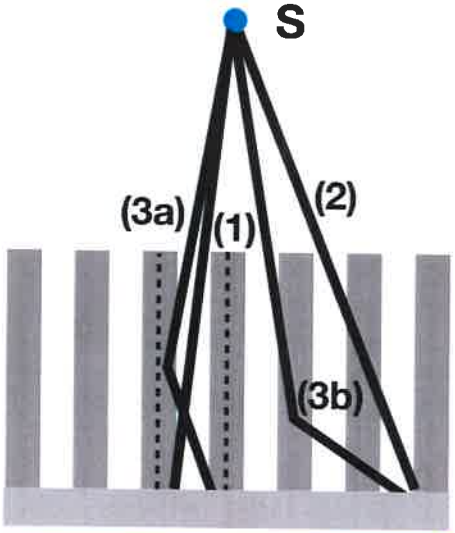


**(1) Geometric Events**

**(2) Penetration Events**

**(3) Scattered Events**

**Spatial Resolution (SR)**

# Collimator intrinsic properties : Insight

## *Septal Penetration* (**SP**)

$$\frac{\text{Events (2+3b)}}{\text{Detected Events}}$$

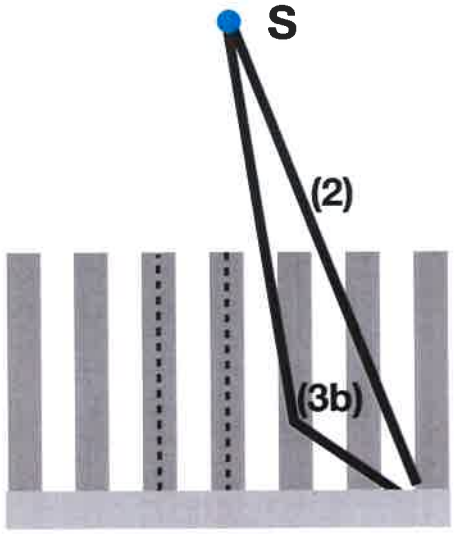


**(2) Penetration Events**

## *Efficiency* (**E**)

$$\frac{\text{Total Events (1+2+3)}}{\text{Emitted Activity}}$$

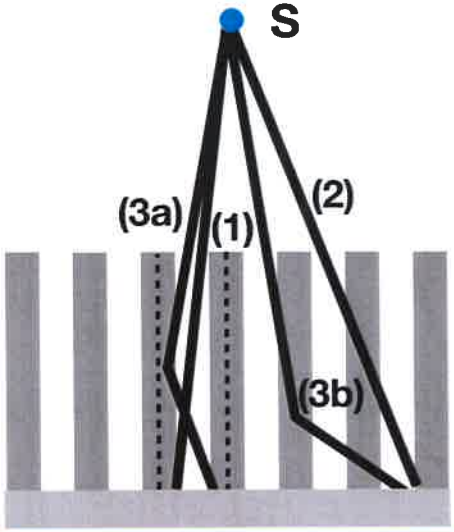


**(1) Geometric Events**

**(2) Penetration Events**

**(3) Scattered Events**

## Spatial *Resolution* (**SR**)

**σ of the sum of profiles inside translated vertical ROI through the line source**

# Collimator intrinsic properties : Insight

## *Septal Penetration* (**SP**)

**Events (2+3b) / Detected Events**

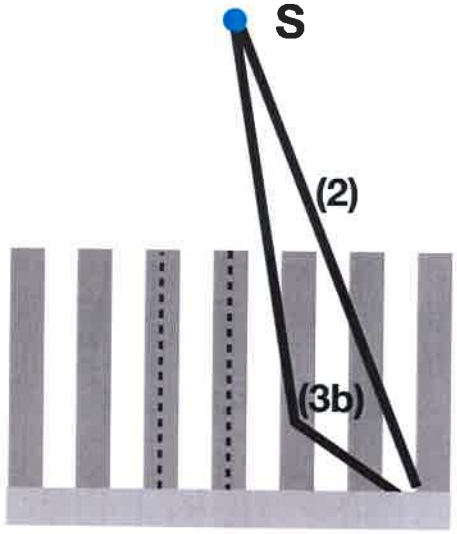


**(2) Penetration Events**

## *Efficiency* (**E**)

**Total Events (1+2+3) / Emitted Activity**

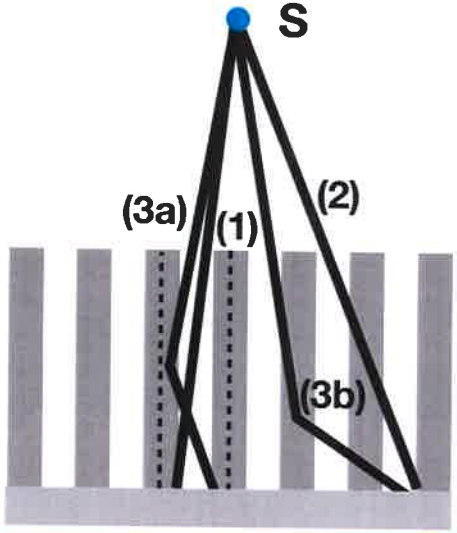


**(1) Geometric Events**

**(2) Penetration Events**

**(3) Scattered Events**

## Spatial *Resolution* (**SR**)

**σ of the sum of profiles inside translated vertical ROI through the line source**

**Useful Events are inside 2σ ROI**

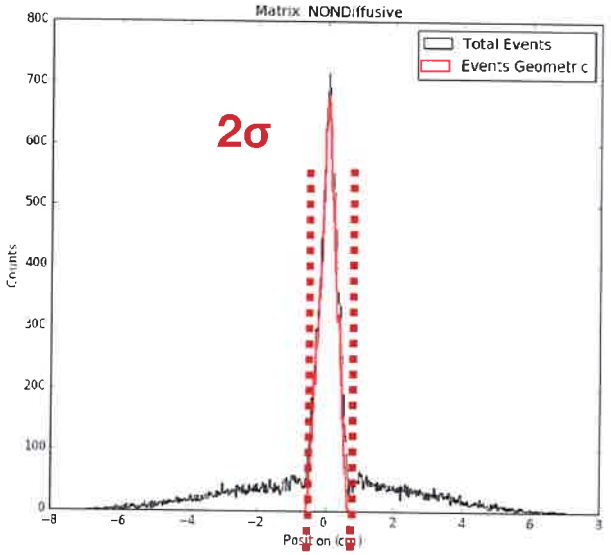

# Collimator intrinsic properties : Insight

## *Septal Penetration* (**SP**)

**Events (2+3b)**

**Detected Events**

## *Effective SP* (**eSP**)

**SP Events outside 2σ**

**Detected Events**

**Events impacting image quality**

## *Efficiency* (**E**)

**Total Events (1+2+3)**

**Emitted Activity**

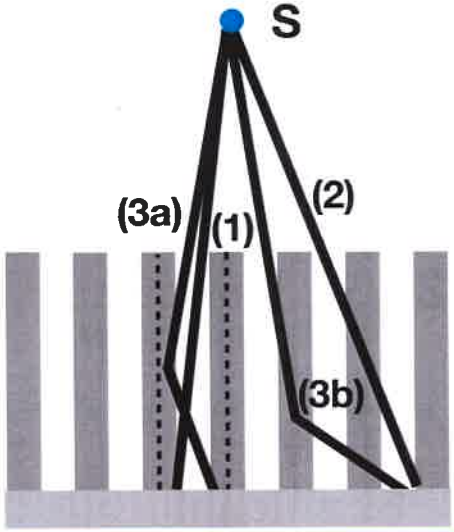


**(1) Geometric Events**

**(2) Penetration Events**

**(3) Scattered Events**

## Spatial *Resolution* (**SR**)

**σ of the sum of profiles inside translated vertical ROI through the line source**

**Useful Events are inside 2σ ROI**

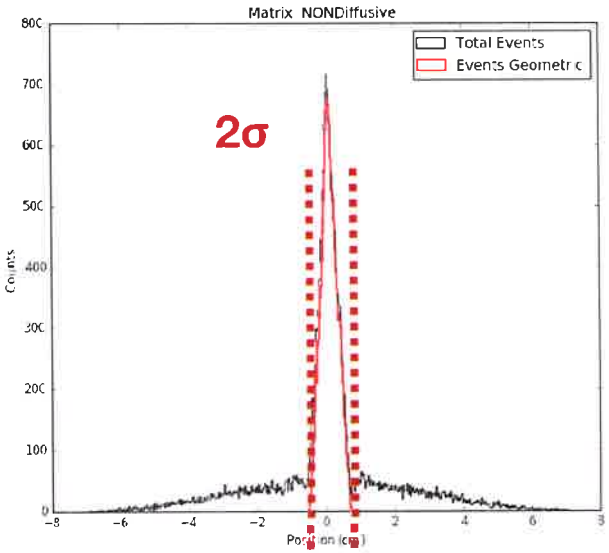

# Collimator intrinsic properties : *SP* and *eSP*

**eSP, Total Events**

L = 3.5 cm

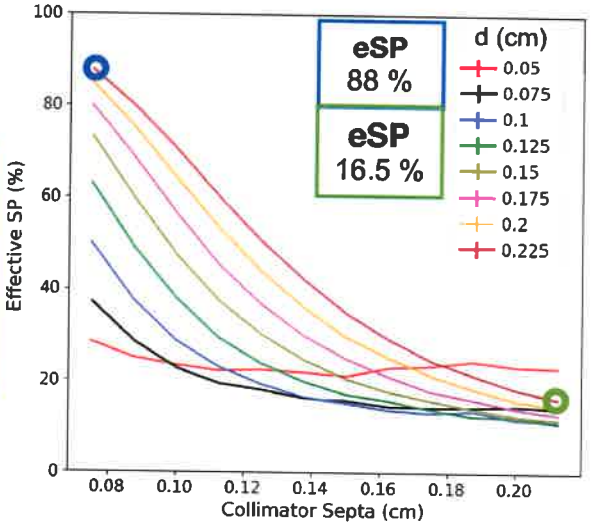


L = 6.5 cm

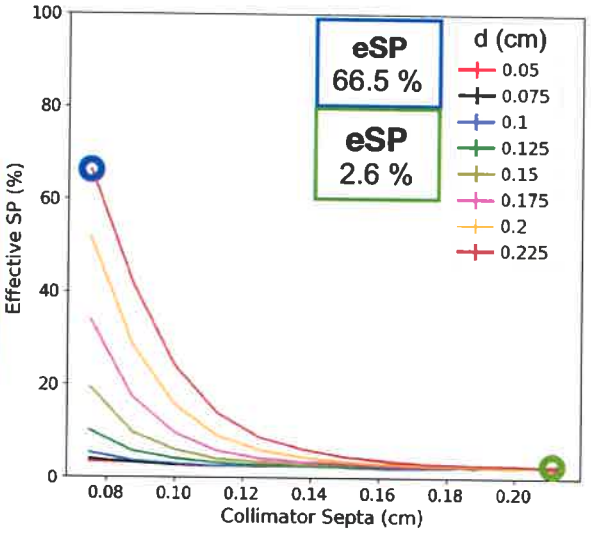

# Collimator intrinsic properties : *SP* and *eSP*

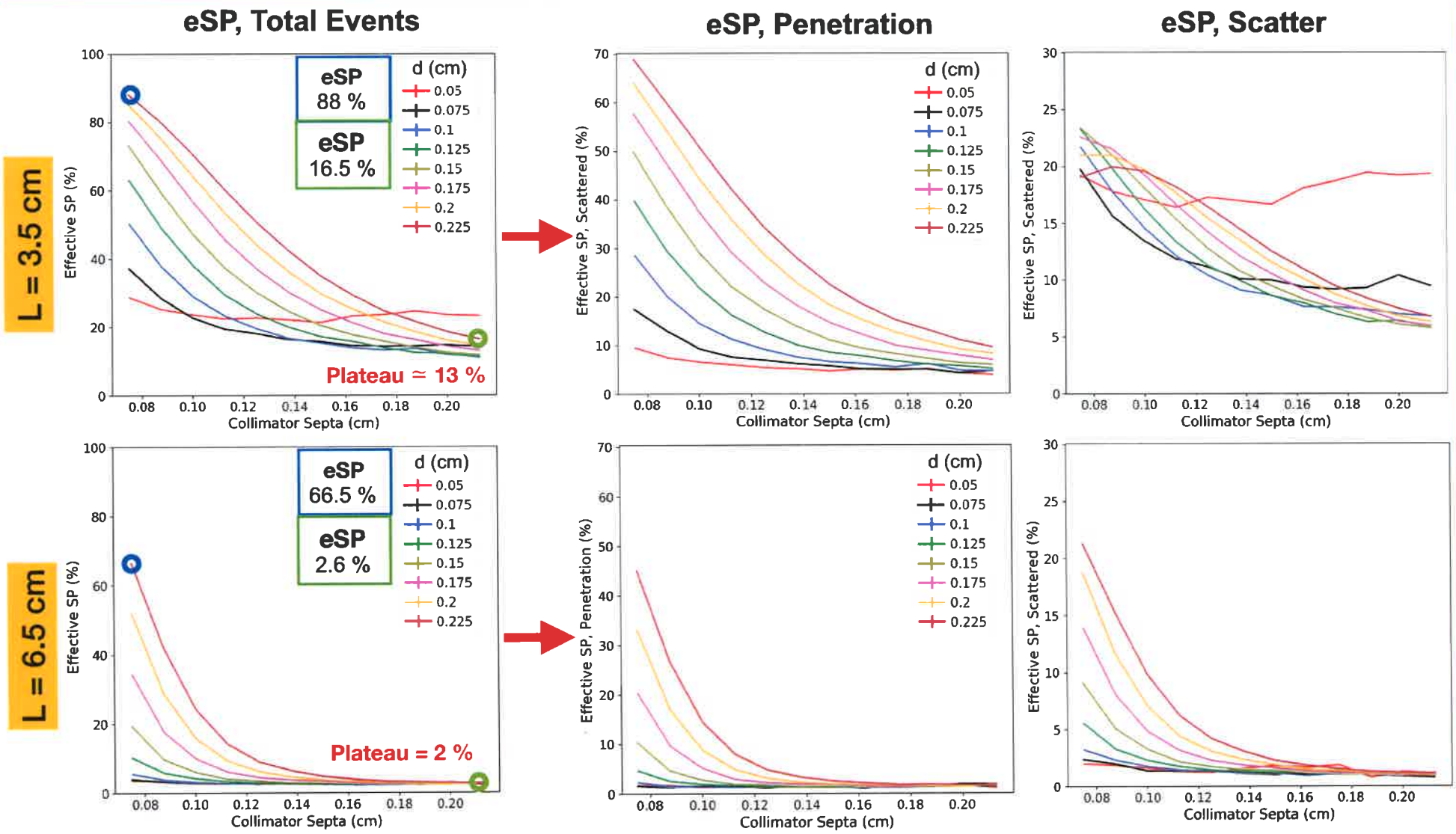


**eSP plateau**

**increase of eSP,S for low d, by increasing t**

# Collimator intrinsic properties : *SP* and *eSP*

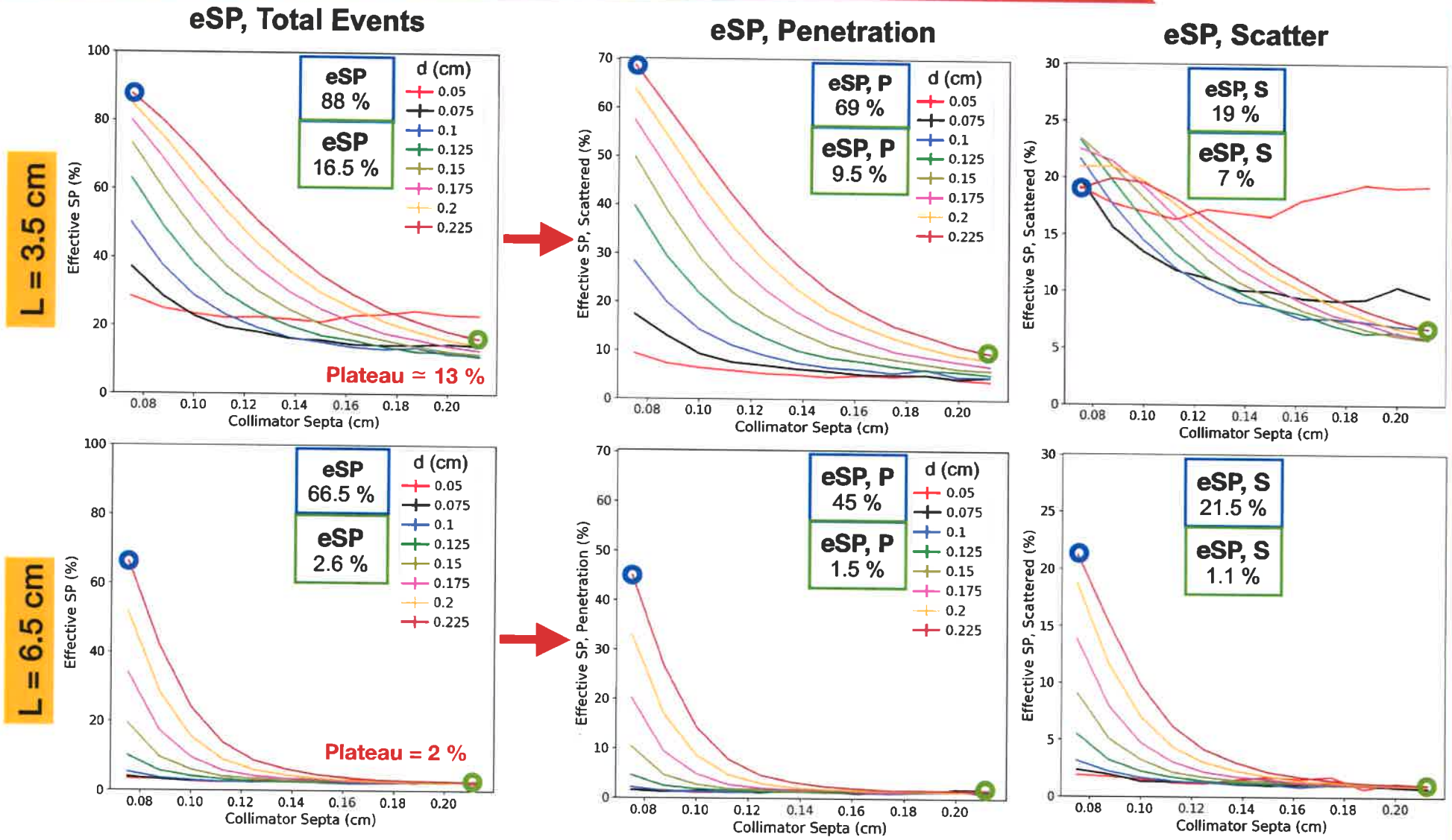


**eSP plateau**

**increase of eSP,S for low d, by increasing t**

# Collimator intrinsic properties : ***SP*** and ***eSP***

**eSP, Total Events** | **eSP, Penetration** | **eSP, Scatter**

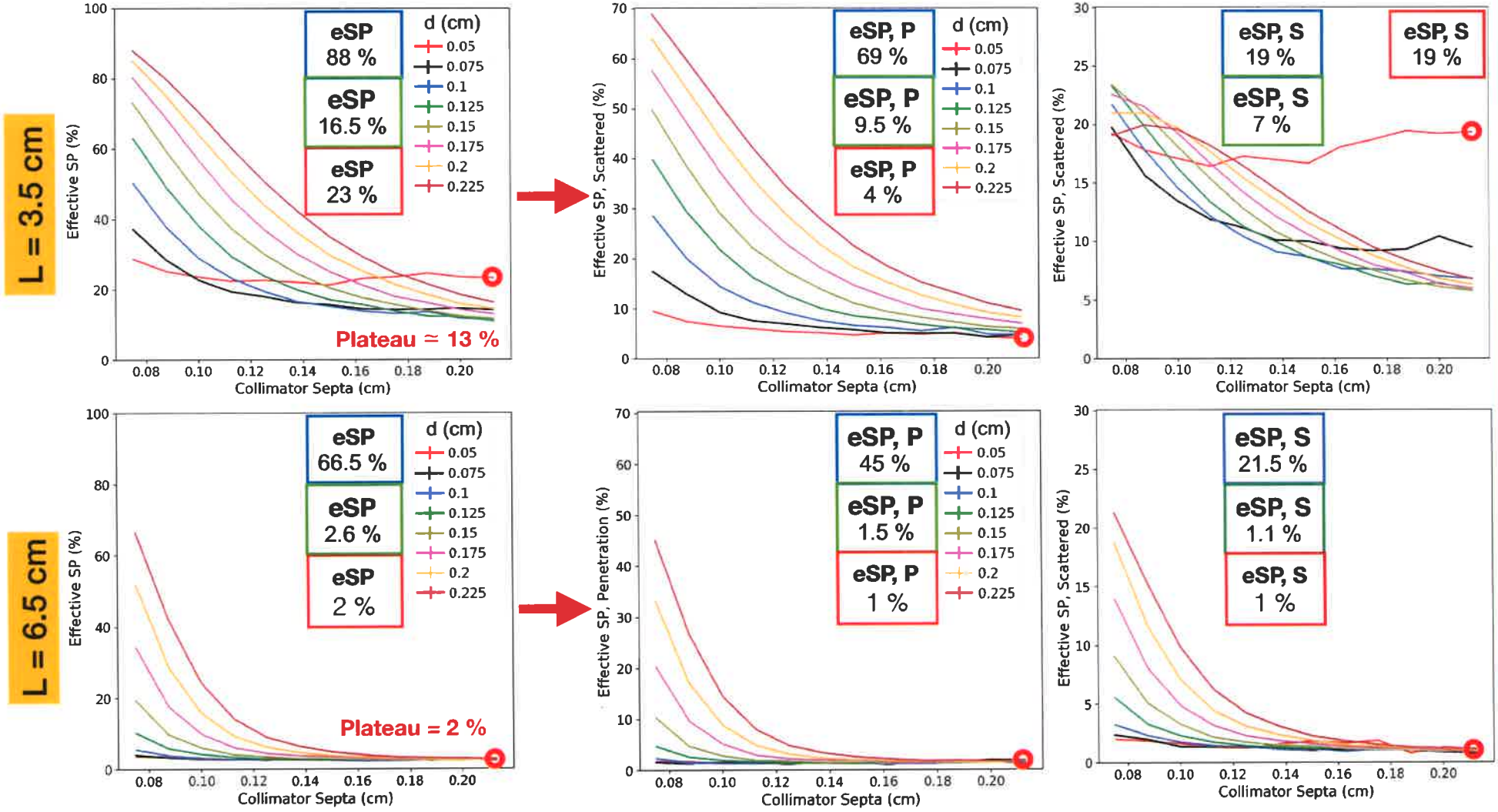


**eSP plateau**

**increase of eSP,S for low d, by increasing t**

# Collimator intrinsic properties : *E*

**L = 3.5 cm**

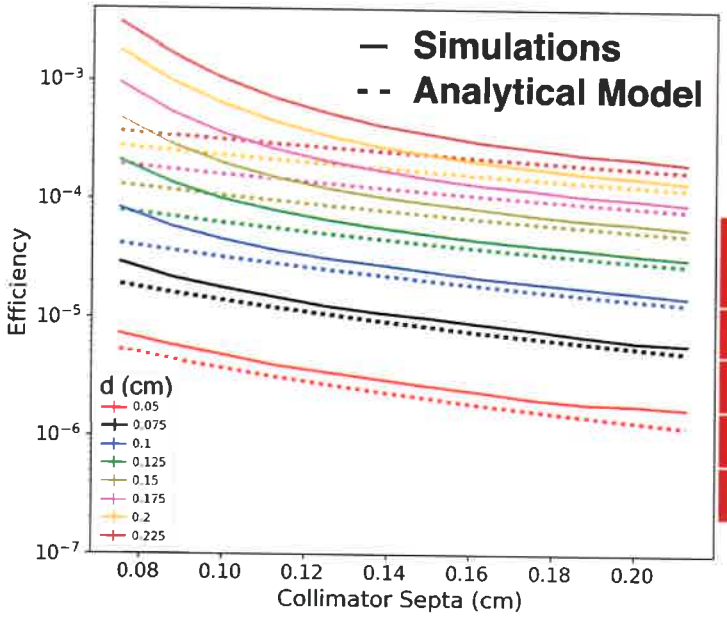


**L = 6.5 cm**

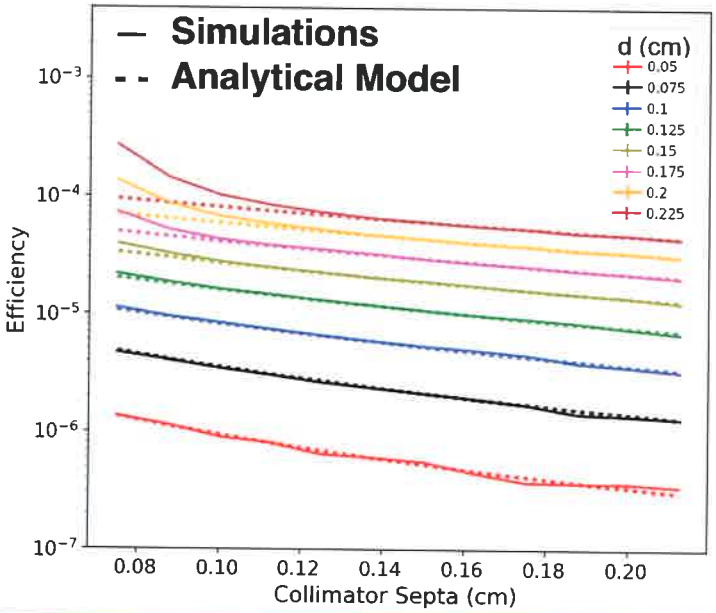


$$E_{th} = K\frac{d^4}{L_e^2(d+t)^2} \qquad L_e = L - \frac{2}{\mu(364keV)}$$

| L (cm) | D (cm) | t (cm) | E (x10⁻⁴) | $E_{th}$ (x10⁻⁴) | eSP (%) | Geometric % | Penetration % | Scattered % |
|---|---|---|---|---|---|---|---|---|
| 3,5 | 0,225 | 0,075 | 31 | 3.8 | 88 | 10.1 | 70.2 | 19.8 |
| 3,5 | 0,225 | 0,225 | 2.0 | 1.77 | 16.5 | 74.9 | 14.5 | 10.6 |
| 6,5 | 0,225 | 0,075 | 2.71 | 0.96 | 66.5 | 31.0 | 46.2 | 22.7 |
| 6,5 | 0,225 | 0,225 | 0.447 | 0.449 | 2.6 | 90.3 | 5.0 | 4.7 |

# Collimator intrinsic properties : *E*

L = 3.5 cm

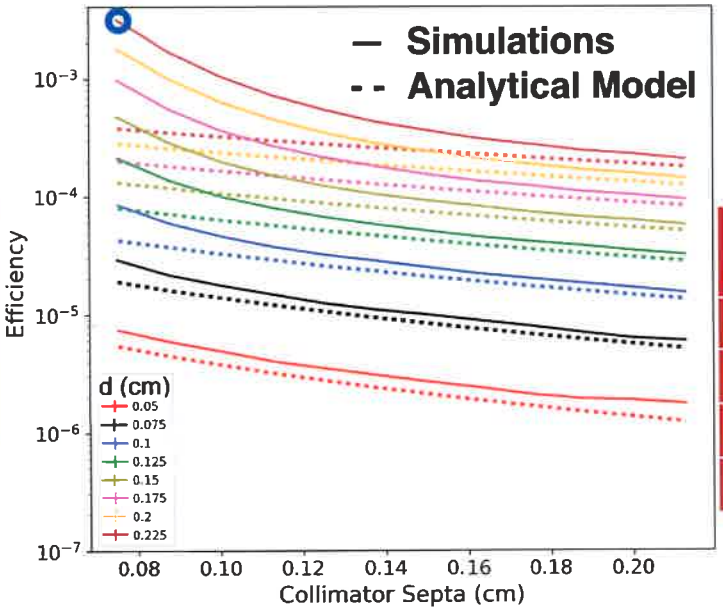


$$E_{th} = K\frac{d^4}{L_e^2(d+t)^2} \qquad L_e = L - \frac{2}{\mu(364keV)}$$

| L (cm) | D (cm) | t (cm) | E (x10⁻⁴) | $E_{th}$ (x10⁻⁴) | eSP (%) | Geometric % | Penetration % | Scattered % |
|---|---|---|---|---|---|---|---|---|
| 3,5 | 0,225 | 0,075 | 31 | 3.8 | 88 | 10.1 | 70.2 | 19.8 |
| 3,5 | 0,225 | 0,225 | 2.0 | 1.77 | 16.5 | 74.9 | 14.5 | 10.6 |
| 6,5 | 0,225 | 0,075 | 2.71 | 0.96 | 66.5 | 31.0 | 46.2 | 22.7 |
| 6,5 | 0,225 | 0,225 | 0.447 | 0.449 | 2.6 | 90.3 | 5.0 | 4.7 |

**with high septal penetration** → **huge increasing of the E**

**E non-predictable using the analytical model**

L = 6.5 cm

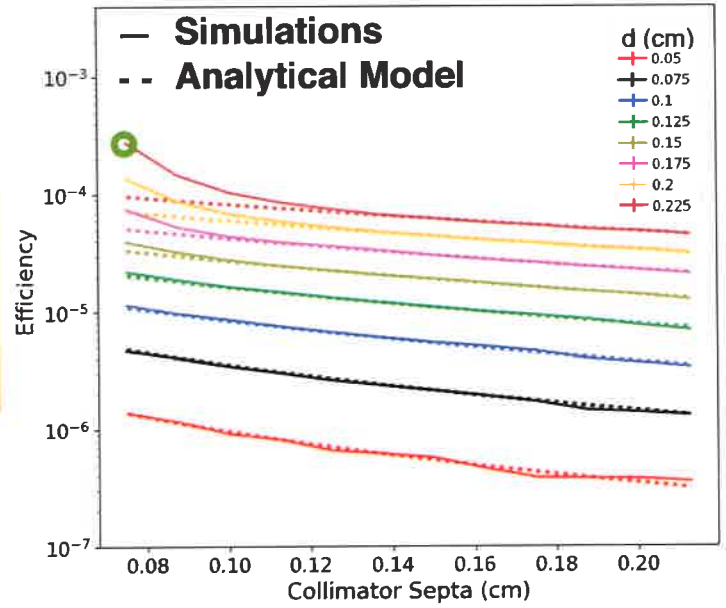

# Collimator intrinsic properties : *E*

**L = 3.5 cm**

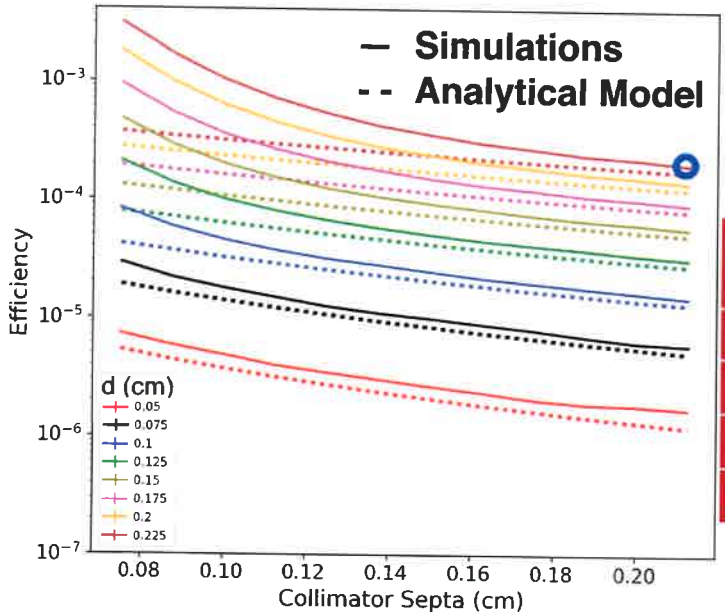


**L = 6.5 cm**

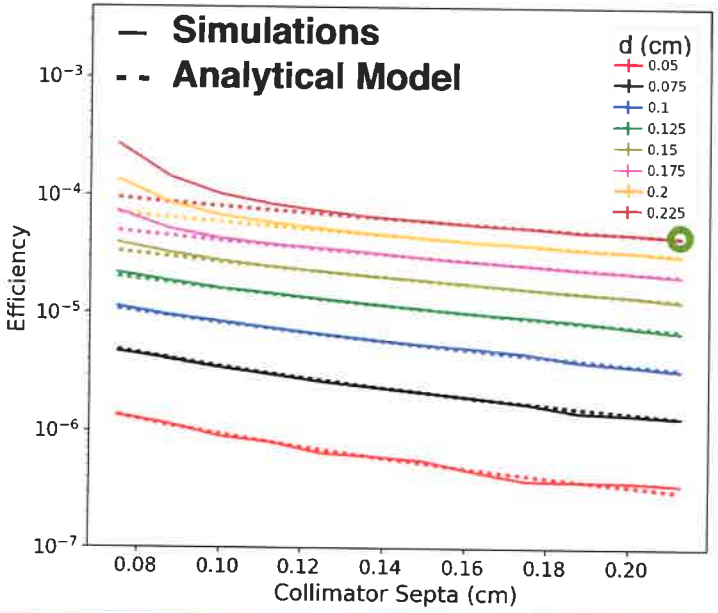


$$E_{th} = K\frac{d^4}{L_e^2(d+t)^2} \qquad L_e = L - \frac{2}{\mu(364keV)}$$

| L (cm) | D (cm) | t (cm) | E (x10$^{-4}$) | $E_{th}$ (x10$^{-4}$) | eSP (%) | Geometric % | Penetration % | Scattered % |
|---|---|---|---|---|---|---|---|---|
| 3,5 | 0,225 | 0,075 | 31 | 3.8 | 88 | 10.1 | 70.2 | 19.8 |
| 3,5 | 0,225 | 0,225 | 2.0 | 1.77 | 16.5 | 74.9 | 14.5 | 10.6 |
| 6,5 | 0,225 | 0,075 | 2.71 | 0.96 | 66.5 | 31.0 | 46.2 | 22.7 |
| 6,5 | 0,225 | 0,225 | 0.447 | 0.449 | 2.6 | 90.3 | 5.0 | 4.7 |

**with high septal penetration** → **huge increasing of the E**

**E non-predictable using the analytical model**

**with lower septal penetration** → **E predictable using the analytical model if the scatter percentage is low (eSP,S < 10 %)**

# Collimator intrinsic properties : *E*

**L = 3.5 cm**

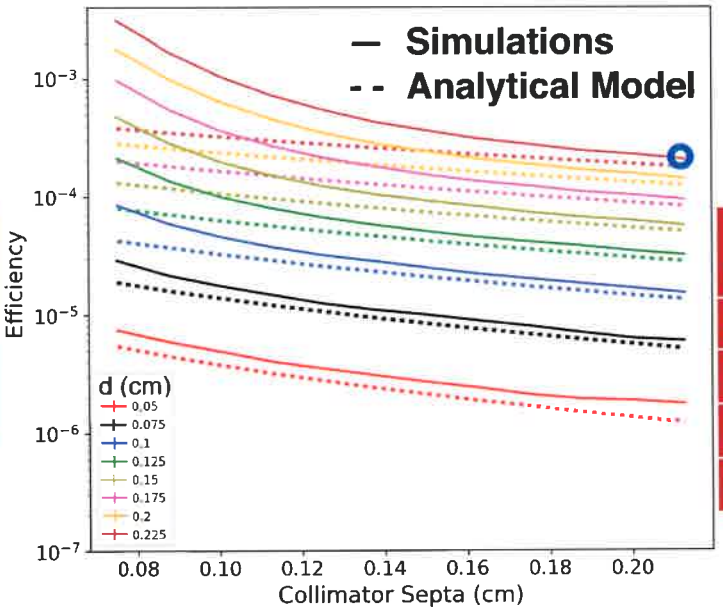


**L = 6.5 cm**

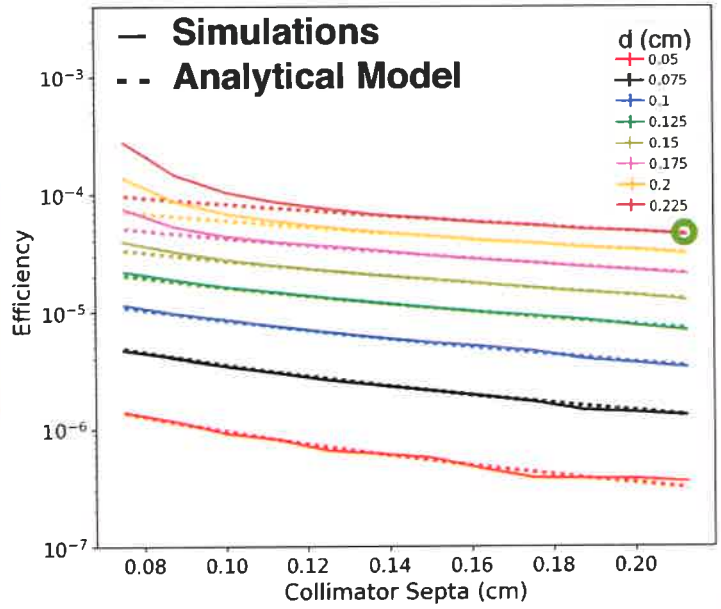


$$E_{th} = K\frac{d^4}{L_e^2(d+t)^2} \qquad L_e = L - \frac{2}{\mu(364keV)}$$

| L (cm) | D (cm) | t (cm) | E (x10⁻⁴) | $E_{th}$ (x10⁻⁴) | eSP (%) | Geometric % | Penetration % | Scattered % |
|---|---|---|---|---|---|---|---|---|
| 3,5 | 0,225 | 0,075 | 31 | 3.8 | 88 | 10.1 | 70.2 | 19.8 |
| 3,5 | 0,225 | 0,225 | 2.0 | 1.77 | 16.5 | 74.9 | 14.5 | 10.6 |
| 6,5 | 0,225 | 0,075 | 2.71 | 0.96 | 66.5 | 31.0 | 46.2 | 22.7 |
| 6,5 | 0,225 | 0,225 | 0.447 | 0.449 | 2.6 | 90.3 | 5.0 | 4.7 |

**with high septal penetration** → **huge increasing of the E**

**E non-predictable using the analytical model**

**with lower septal penetration** → **E predictable using the analytical model if the scatter percentage is low (eSP,S < 10 %)**

**At high energy, simulations are mandatory in order to well estimate the collimator's efficiency**

# Collimator intrinsic properties : ***SR***

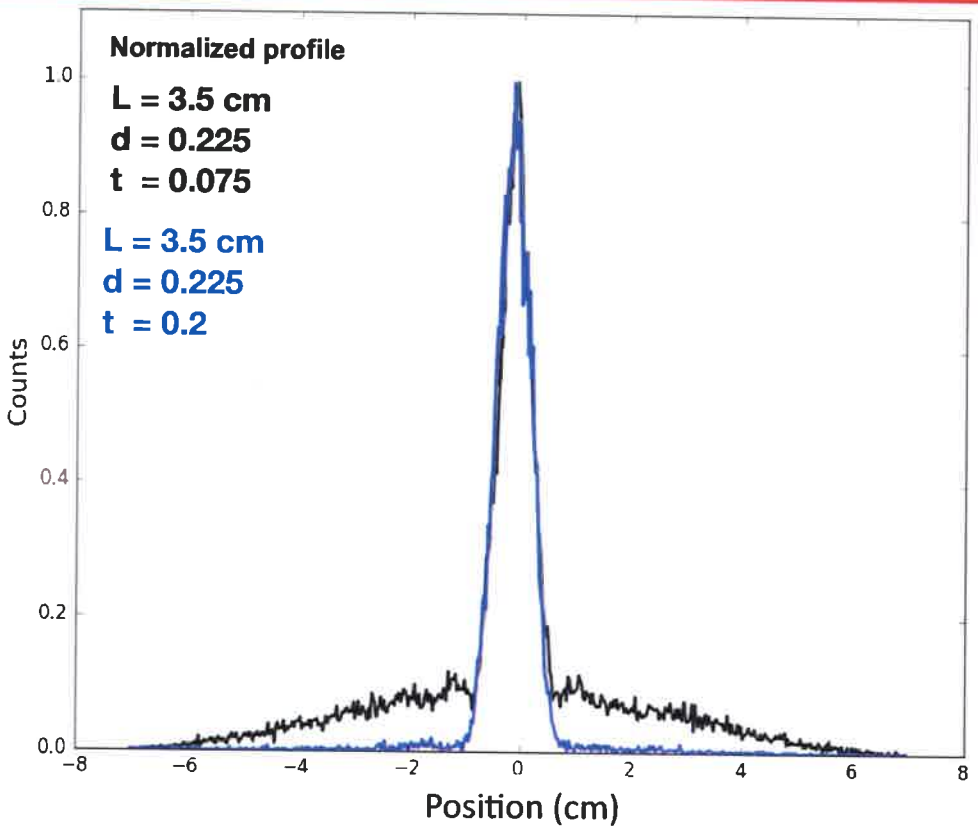


**FWHM**

**independent of the septa**

**not influenced by penetration and scattered events**

# Collimator intrinsic properties : *SR*

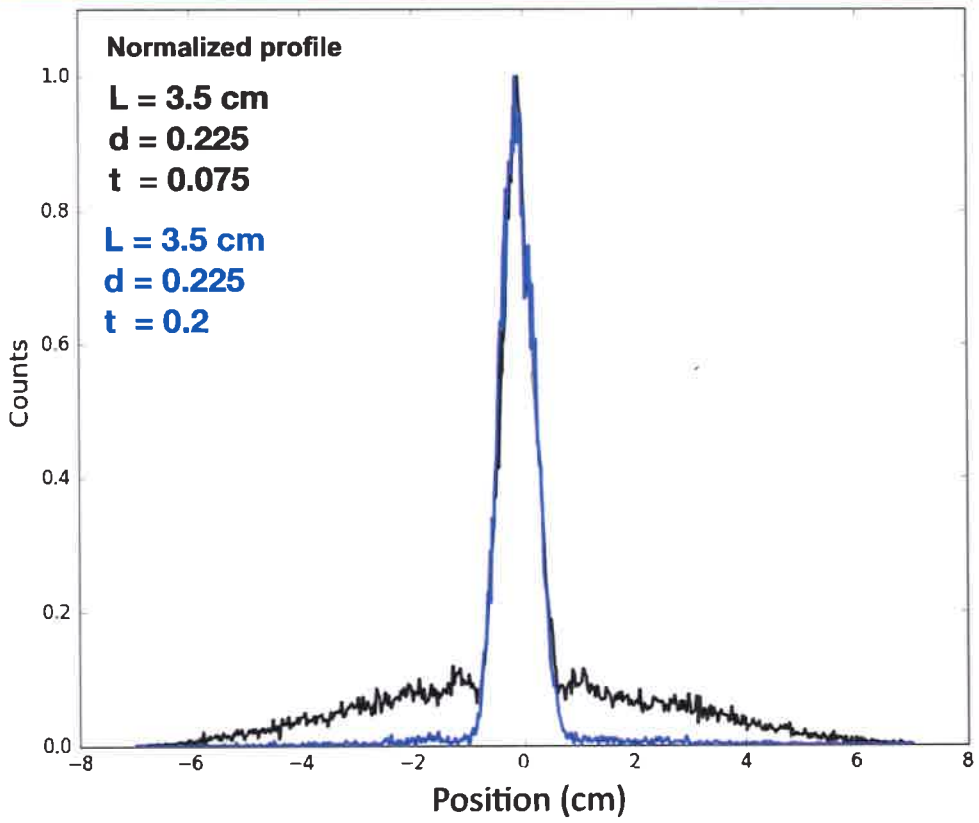


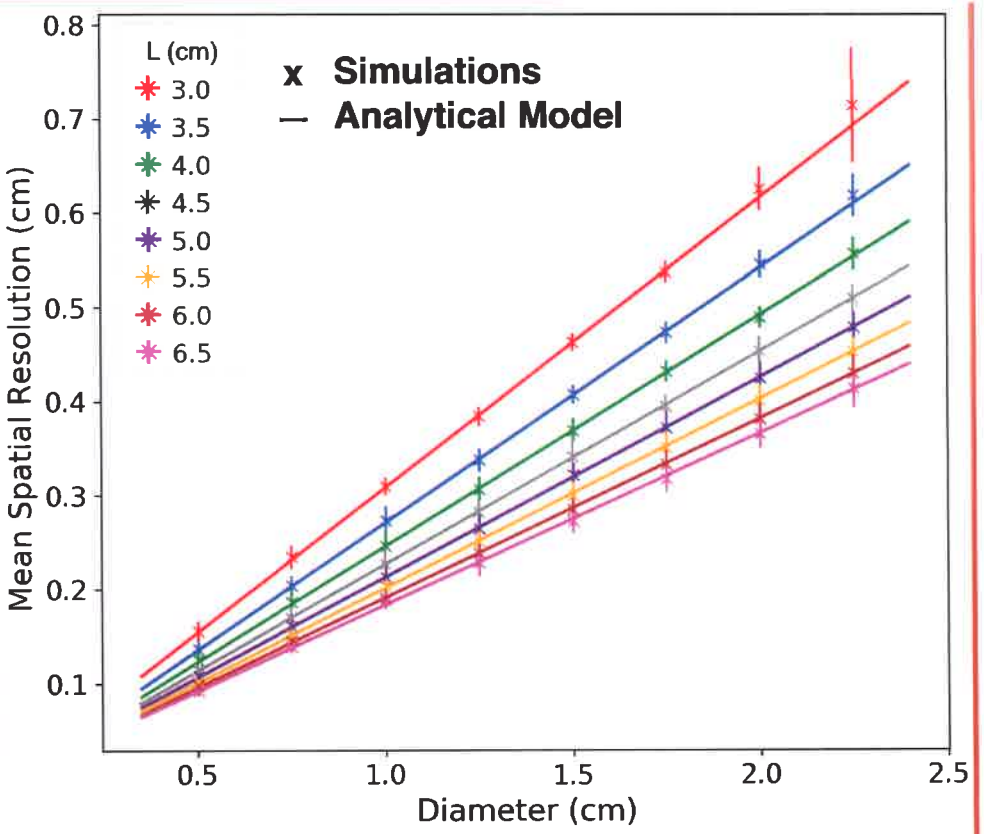


**FWHM**

**independent of the septa**

**not influenced by penetration and scattered events**

$$SR_{th} = \frac{d(L_e+b)}{L_e}$$

**SR is well fitted by the analytical model**

# Configurations choice

**for each L, d configurations extrapolation of the t that allows eSP = 10% @ 5 cm**

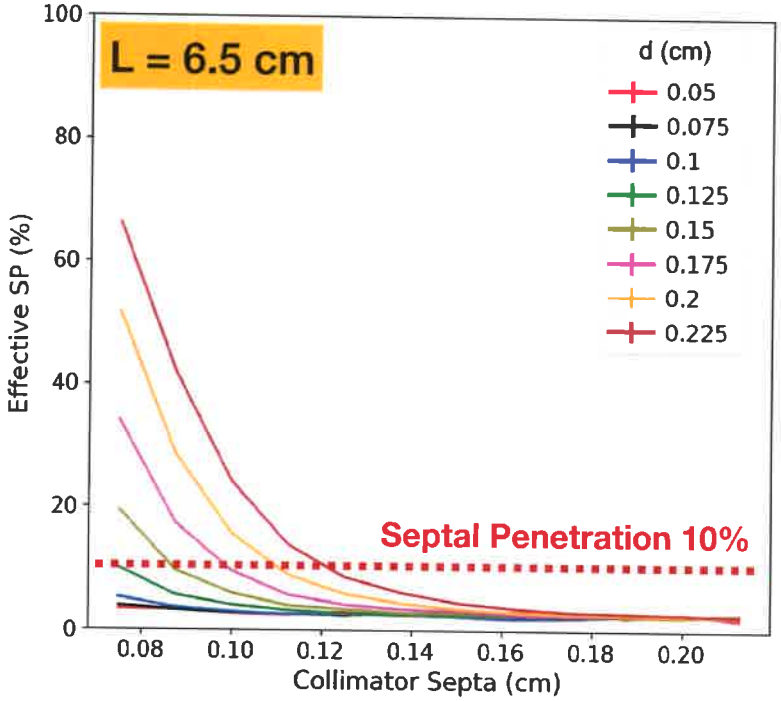

# Configurations choice

**for each L, d configurations extrapolation of the *t* that allows eSP = 10% @ 5 cm**

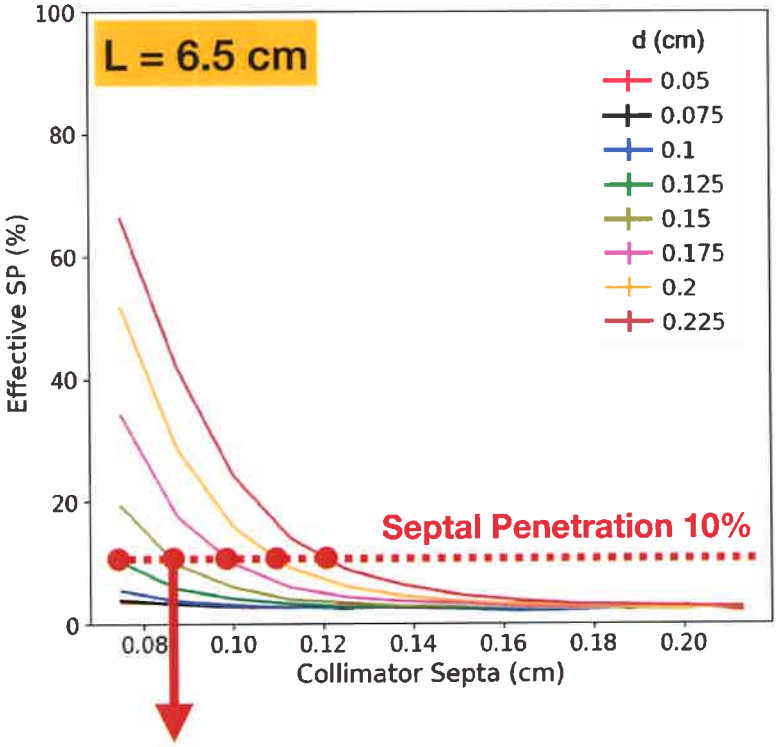


**Example :**
**L = 6.5 cm**
**d = 0.15 cm**
***t* = 0.086**

**new L, d, *t* configurations with eSP=10% !**

# Configurations choice

**for each L, d configurations extrapolation of the *t* that allows eSP = 10% @ 5 cm**

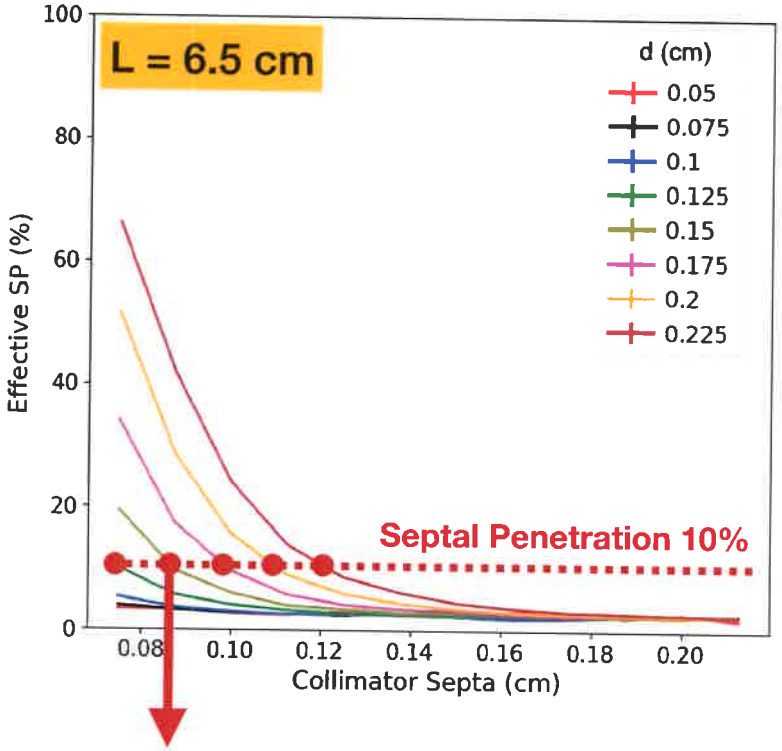


**Example :**
**L = 6.5 cm**
**d = 0.15 cm**
***t* = 0.086**

**new L, d, *t* configurations with eSP=10% !**

**interpolation to obtain other diameters**

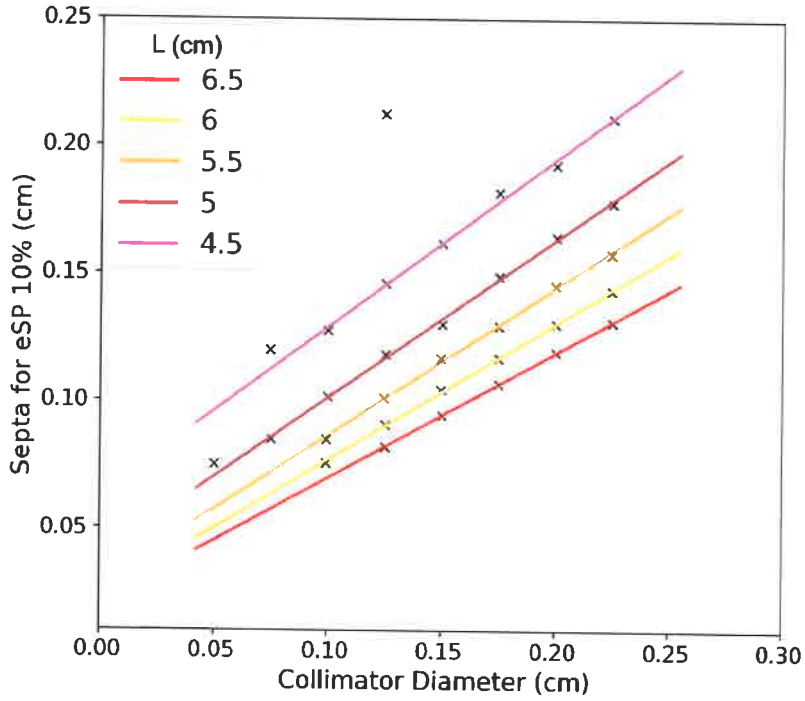

# Configurations choice

**for each L, d configurations extrapolation of the *t* that allows eSP = 10% @ 5 cm**

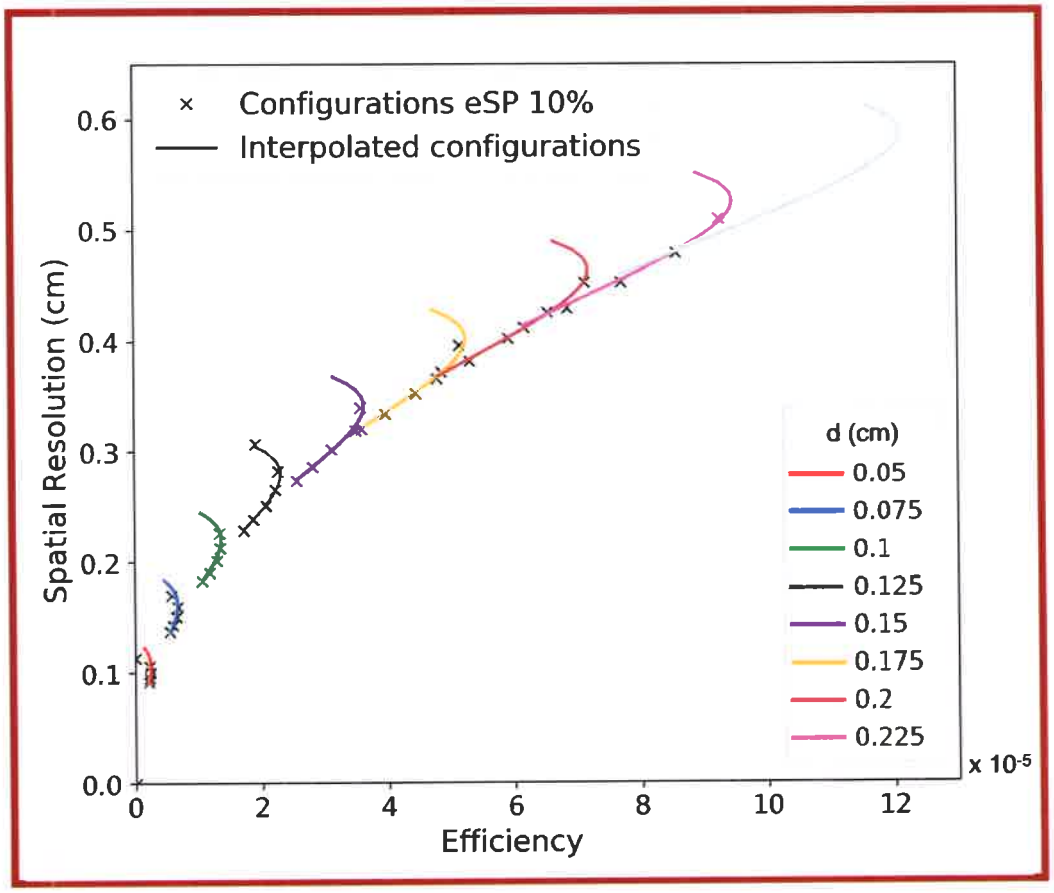


**interpolation to obtain other diameters**

**new L,d,t configurations (eSP=10%) used as input in the analytical model to obtain SR and E**

# Configurations choice

**for each L, d configurations extrapolation of the *t* that allows eSP = 10% @ 5 cm**

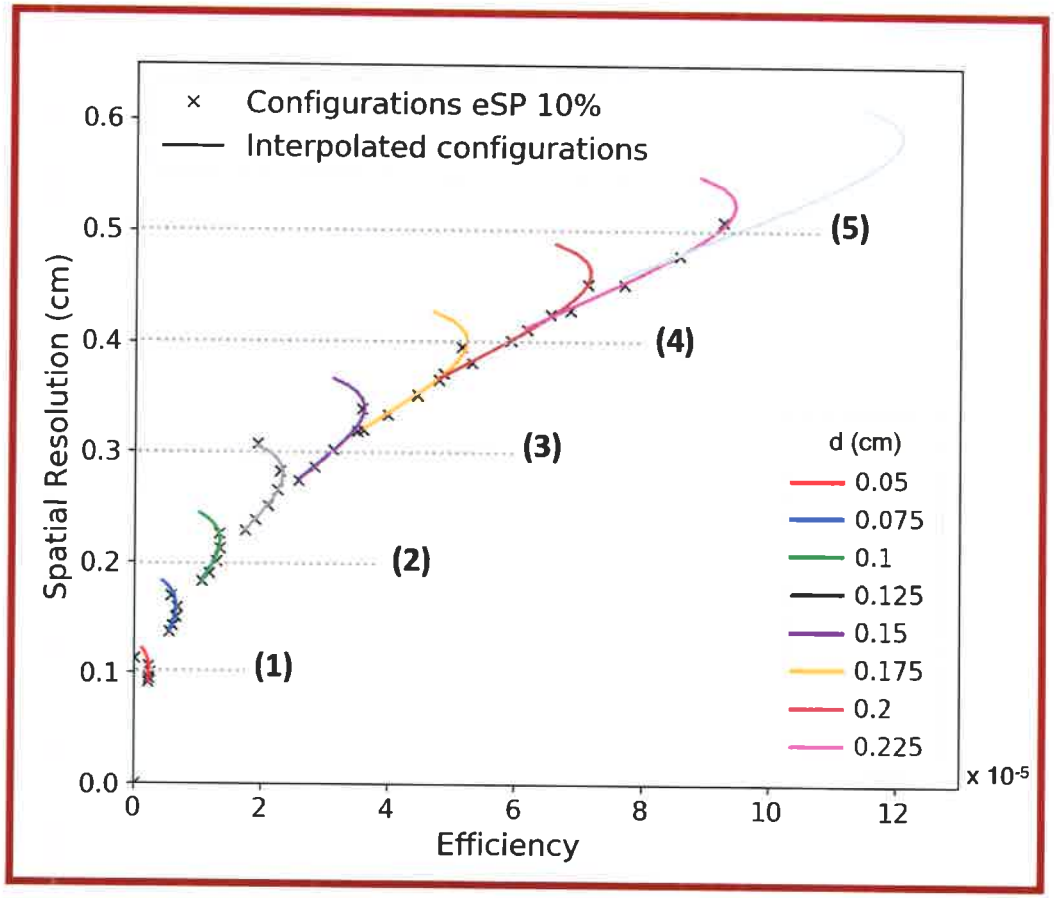


**interpolation to obtain other diameters**

**new L,d,t configurations (eSP=10%) used as input in the analytical model to obtain SR and E**

**SR ∈ [1,5] mm**

| L = 5,5 cm | (1) | (2) | (3) | (4) | (5) |
|---|---|---|---|---|---|
| d (cm) | 0,05 | 0,1 | 0,15 | 0,2 | 0,25 |
| t (cm) | 0,055 | 0,085 | 0,115 | 0,145 | 0,175 |
| SR @ 5 cm (mm) | 1 | 2 | 3 | 4 | 5 |
| Efficiency @ 5 cm | 0.23 $10^{-5}$ | 1.24 $10^{-5}$ | 3.10 $10^{-5}$ | 5.83 $10^{-5}$ | 9.42 $10^{-5}$ |

# Collimator intrinsic properties with distance

## $^{131}$I cylindrical source in air

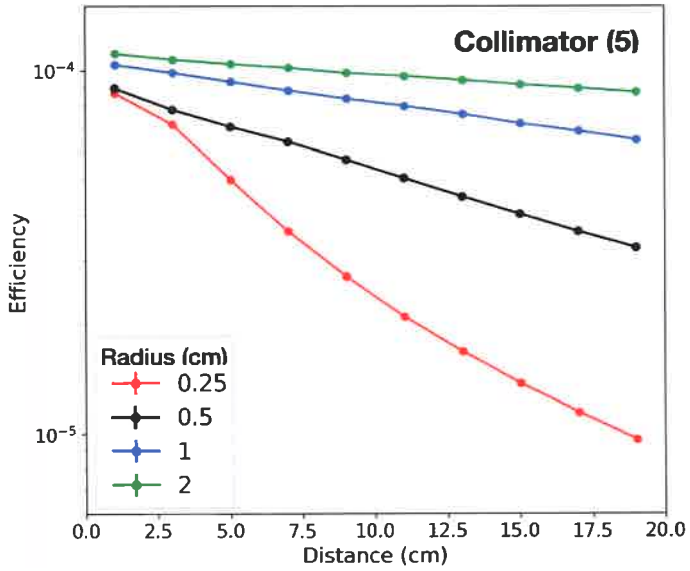


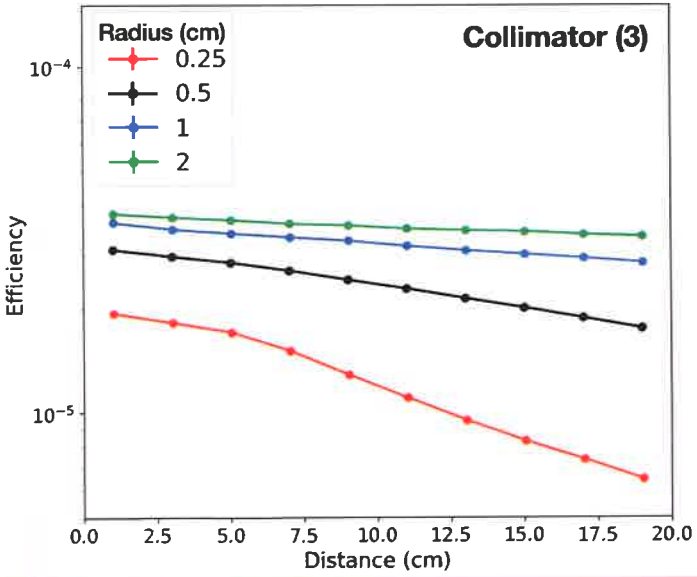

# Collimator intrinsic properties with distance

## $^{131}$I cylindrical source in air

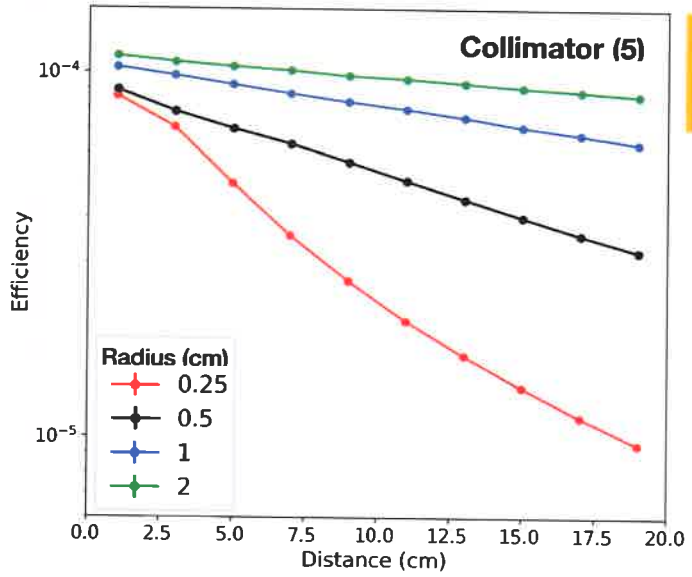


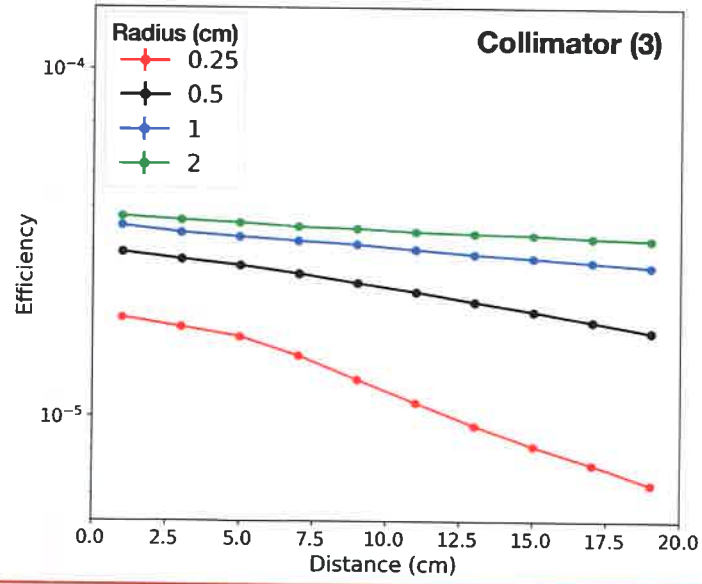


## Efficiency in ROIs = Radius

| decrease with distance | lower for smaller source | decrease faster for smaller source |
|---|---|---|

# Collimator intrinsic properties with distance

## $^{131}$I cylindrical source in air

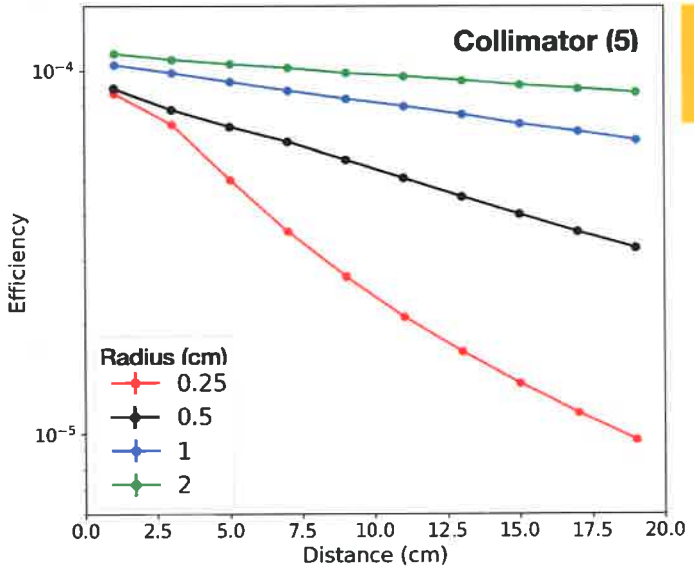


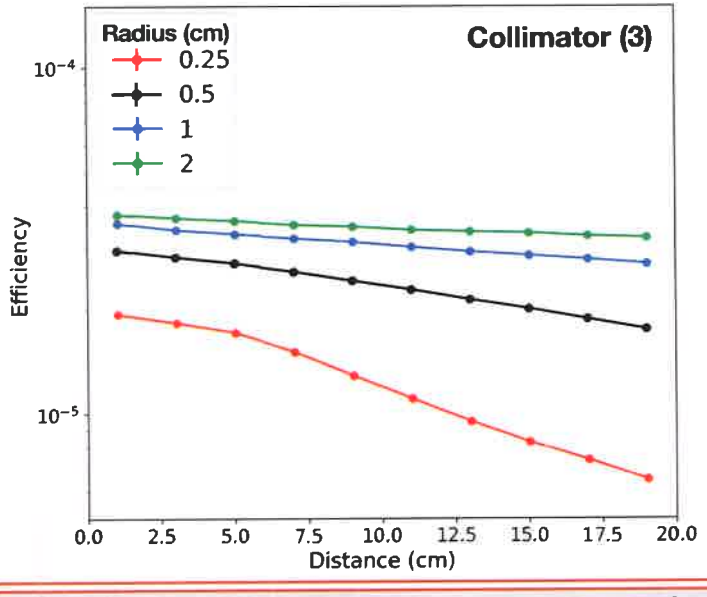


## Efficiency in ROIs = Radius

| decrease with distance | lower for smaller source | decrease faster for smaller source |
|---|---|---|

## E in all FoV

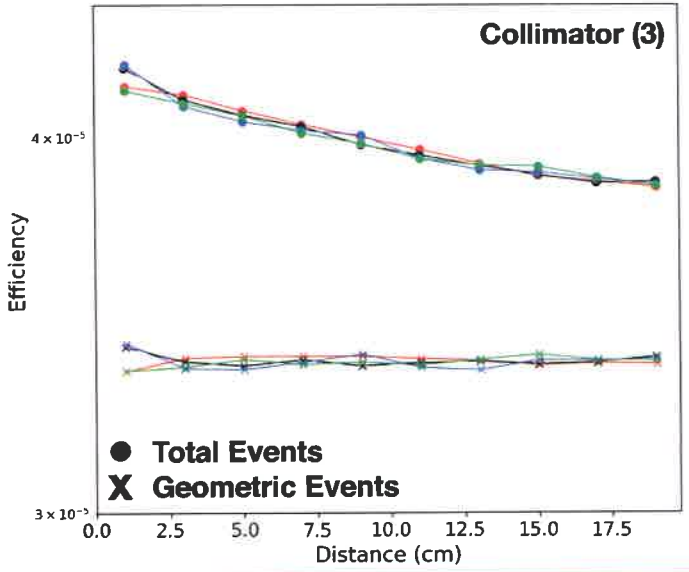

# Collimator intrinsic properties with distance

## $^{131}$I cylindrical source in air

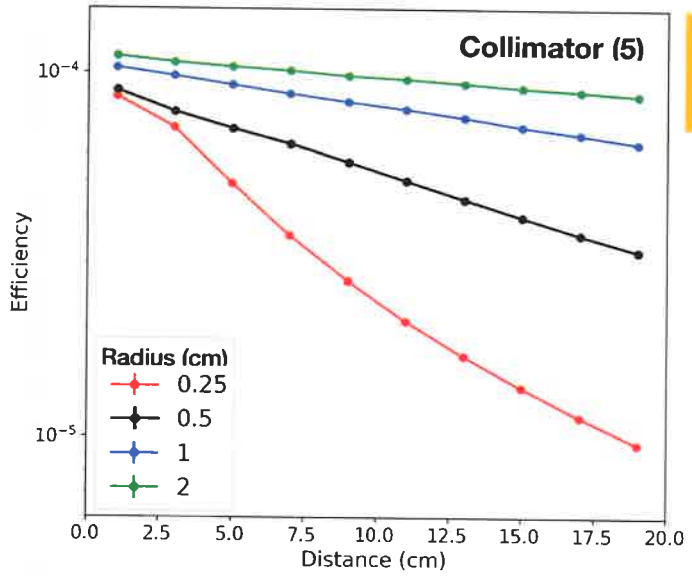


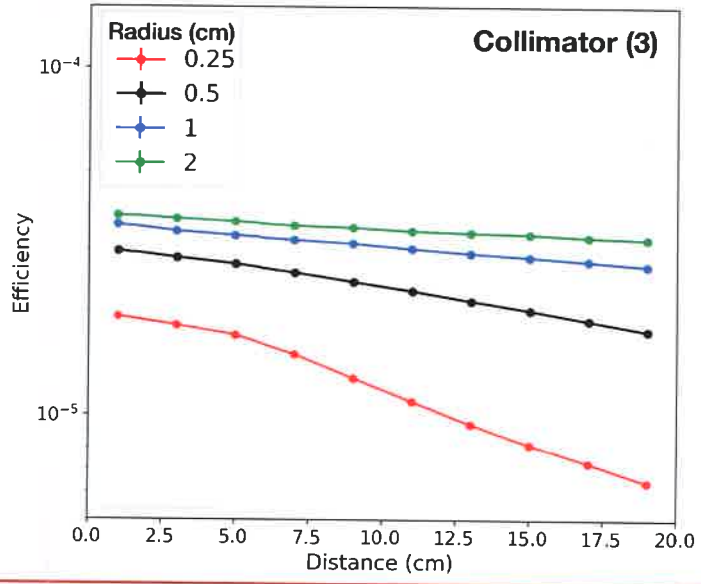


## Efficiency in ROIs = Radius

**decrease with distance** | **lower for smaller source** | **decrease faster for smaller source**

**SR value increases with distance**

**Penetration and Scatter decrease with distance**

## E in all FoV

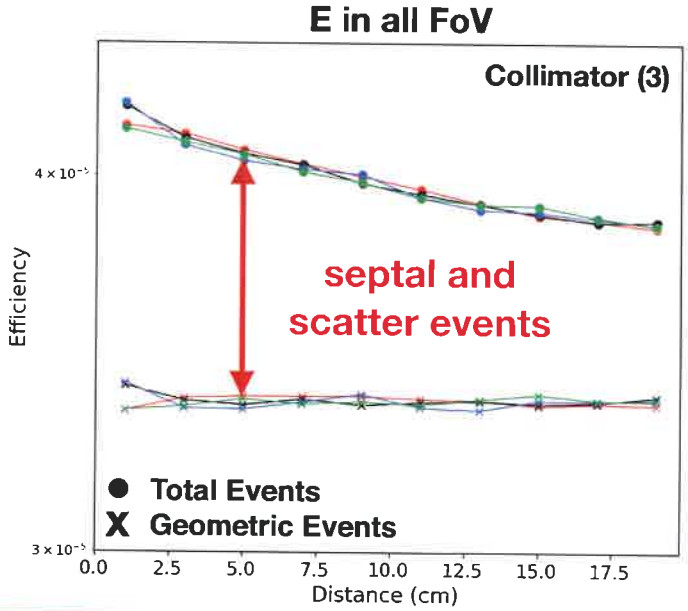

# Collimator intrinsic properties with distance

## $^{131}$I cylindrical source in air

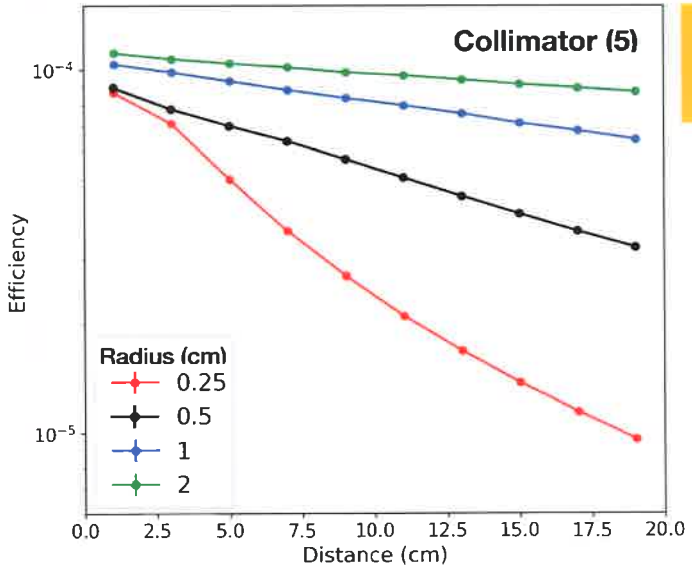


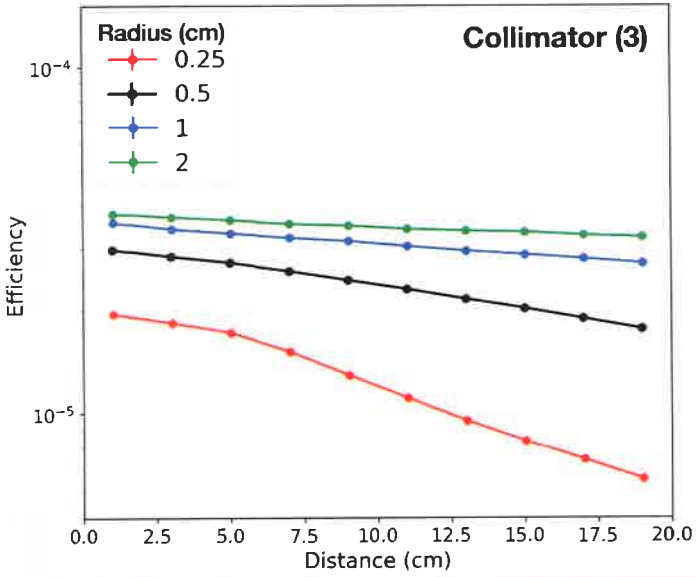


## Efficiency in ROIs = Radius

**decrease with distance** | **lower for smaller source** | **decrease faster for smaller source**

**SR value increases with distance**

**Penetration and Scatter decrease with distance**

**Partial Volume Effect**

**E in all FoV**

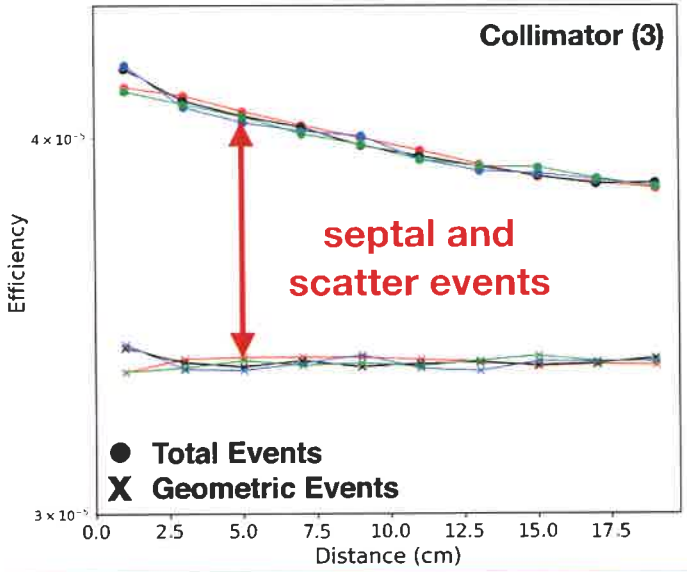

# Complete camera in a real clinical context

## XCAT VOXELIZED PHANTOM

**HEAD**

**3 mm³**

**NECK**

**1 mm³**

**BODY**

**3 mm³**

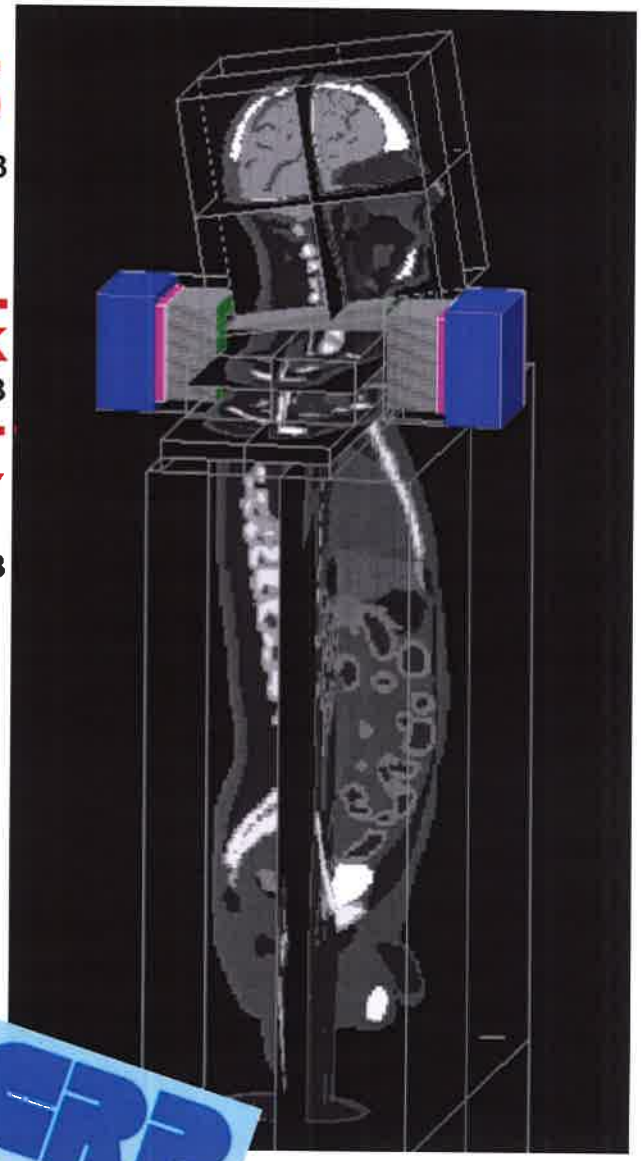

ICRP Annals of the ICRP

# Complete camera in a real clinical context

## XCAT VOXELIZED PHANTOM

**HEAD**

**3 mm³**

**NECK**

**1 mm³**

**BODY**

**3 mm³**

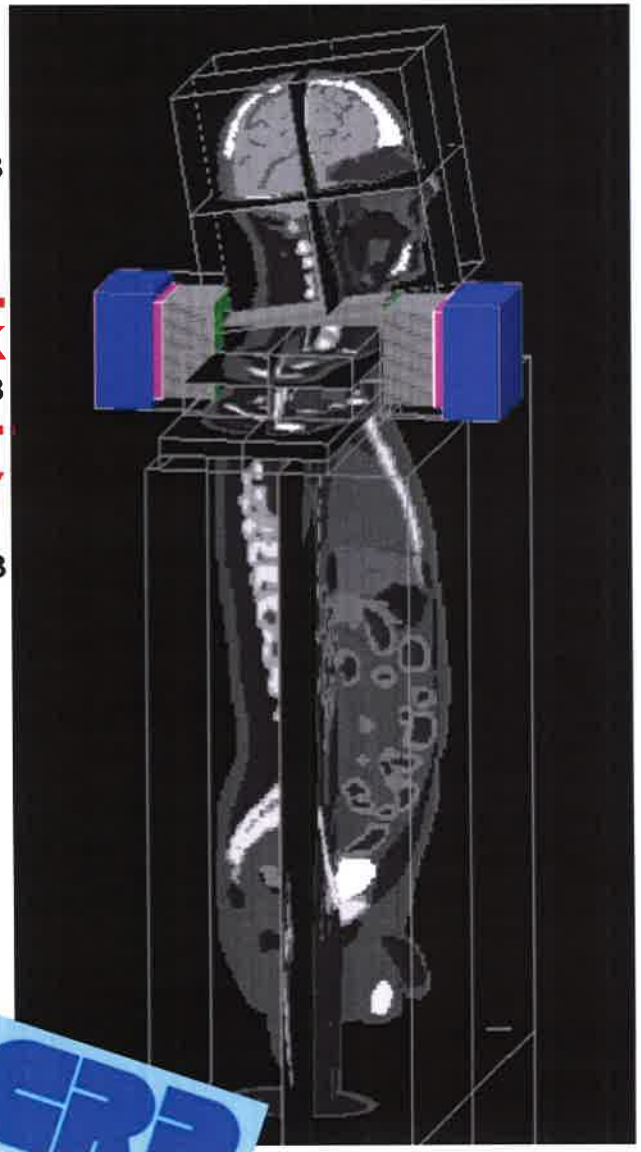

## 2 complete cameras in conjugate view

Fundamental for imaging quantification [1],[2]


*[1] "MIRD pamphlet No. 24: Guidelines for quantitative 131I SPECT in dosimetry applications.", (2013), Dewaraja,et al.*

*[2] "MIRD pamphlet no. 16: techniques for quantitative radiopharmaceutical biodistribution data acquisition and analysis for use in human radiation dose estimates.", (1999), Siegel et al.*


ICRP Annals of the ICRP

# Complete camera in a real clinical context

## XCAT VOXELIZED PHANTOM

**HEAD**
**3 mm³**

**NECK**
**1 mm³**

**BODY**
**3 mm³**

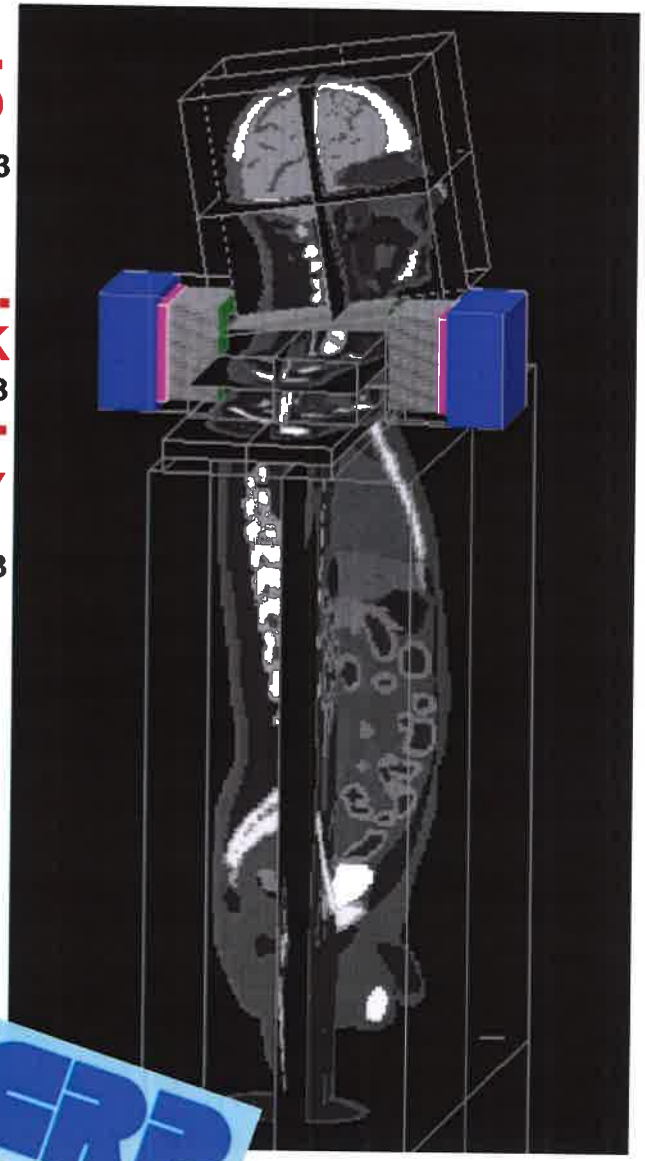

**2 complete cameras in conjugate view**

Fundamental for imaging quantification [1],[2]

**Common hyperthyroidism features**

Thyroid and Nodules dimension [3]

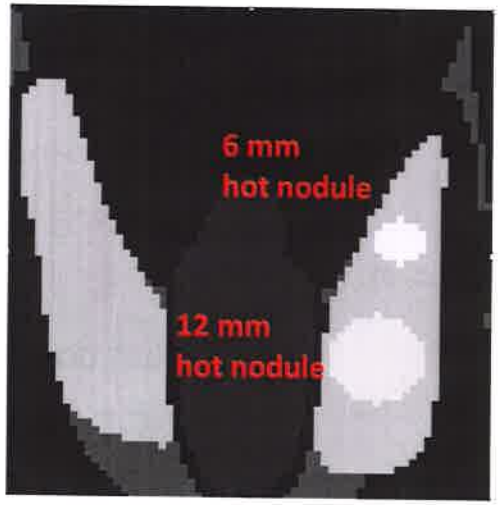


**Neck Phantom's Slice**


*[1] "MIRD pamphlet No. 24: Guidelines for quantitative 131I SPECT in dosimetry applications.", (2013), Dewaraja,et al.*

*[2] "MIRD pamphlet no. 16: techniques for quantitative radiopharmaceutical biodistribution data acquisition and analysis for use in human radiation dose estimates.", (1999), Siegel et al.*

*[3] "Evaluation of dosimetry of radioiodine therapy in benign and malignant thyroid disorders by means of iodine124 and PET." European journal of nuclear medicine and molecular imaging, (2002), Eschmann et al.*


ICRP Annals of the ICRP

# Complete camera in a real clinical context

## XCAT VOXELIZED PHANTOM

HEAD
3 mm³

NECK
1 mm³

BODY
3 mm³

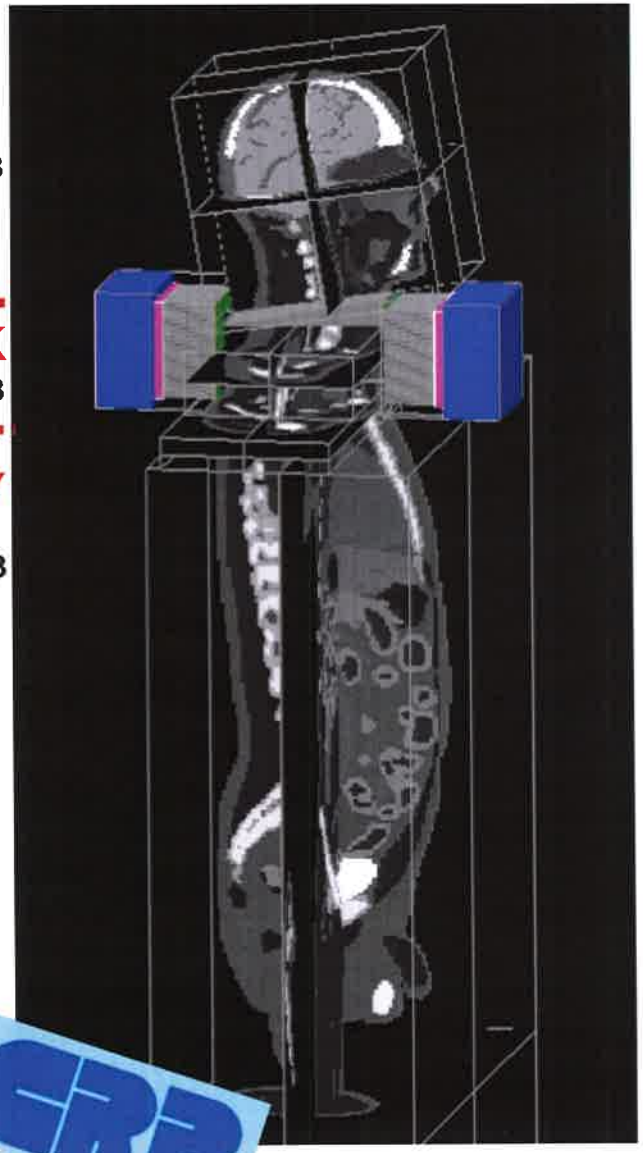

**2 complete cameras in conjugate view**

Fundamental for imaging quantification [1],[2]

**Common hyperthyroidism features**

Thyroid and Nodules dimension [3]

**Real Clinical Practices**

| | |
|---|---|
| Real Mean Injected activity | **300 MBq** [4],[5] |
| Common acquisition time | **10 min** [4],[5] |


*[1] "MIRD pamphlet No. 24: Guidelines for quantitative 131I SPECT in dosimetry applications.", (2013), Dewaraja,et al.*

*[2] "MIRD pamphlet no. 16: techniques for quantitative radiopharmaceutical biodistribution data acquisition and analysis for use in human radiation dose estimates.", (1999), Siegel et al.*

*[3] "Evaluation of dosimetry of radioiodine therapy in benign and malignant thyroid disorders by means of iodine124 and PET." European journal of nuclear medicine and molecular imaging, (2002), Eschmann et al.*

*[4] "EANM procedure guidelines for therapy of benign thyroid disease." European journal of nuclear medicine and molecular imaging", (2010), Stokkel, et al.*

*[5] "Radioiodine therapy in benign thyroid disorders. Evaluation of French nuclear medicine practices." Annales d'endocrinologie, (2014), Bernard et al.*


ICRP Annals of the ICRP

# Complete camera in a real clinical context

## XCAT VOXELIZED PHANTOM

**HEAD**
**3 mm³**

**NECK**
**1 mm³**

**BODY**
**3 mm³**

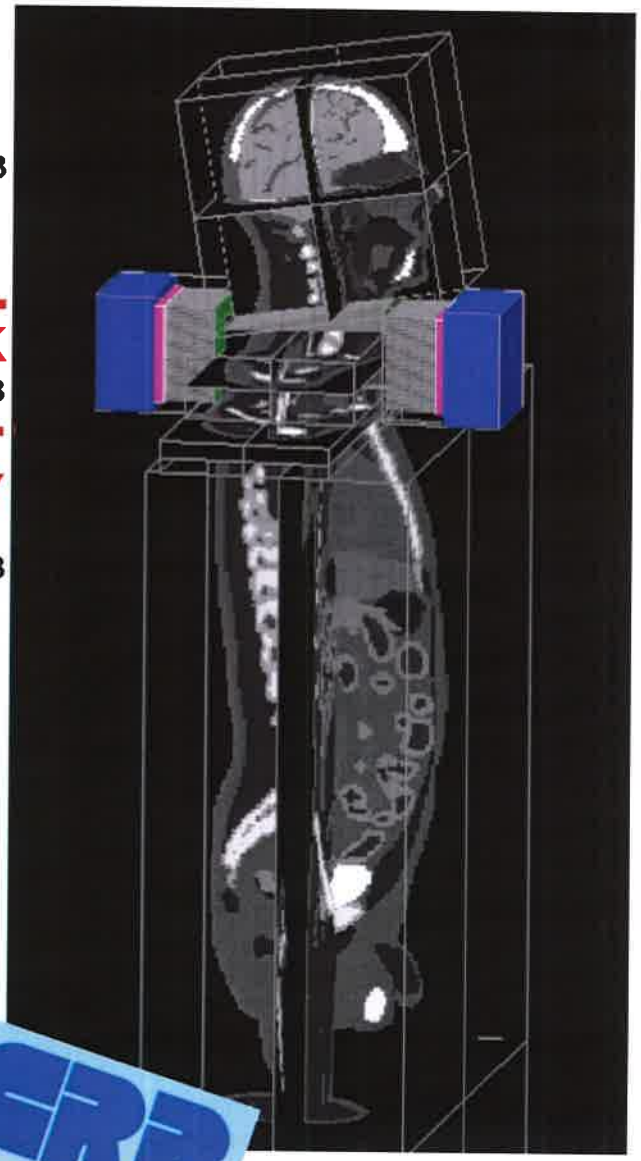

### 2 complete cameras in conjugate view

Fundamental for imaging quantification [1],[2]

### Common hyperthyroidism features

Thyroid and Nodules dimension [3]

### Real Clinical Practices

| | | |
|---|---|---|
| Real Mean Injected activity | **300 MBq** | [4],[5] |
| Common acquisition time | **10 min** | [4],[5] |

### Hyperthyroidism activities distributions at 24h

| | | |
|---|---|---|
| Thyroid uptake | **55 %** | [5],[6] |
| Nodules to Normal Thyroid tissue uptake | **6** | [3] |
| Background using Iodine bio-kinetics model | | [6] |


*[1] "MIRD pamphlet No. 24: Guidelines for quantitative 131I SPECT in dosimetry applications.", (2013), Dewaraja,et al.*

*[2] "MIRD pamphlet no. 16: techniques for quantitative radiopharmaceutical biodistribution data acquisition and analysis for use in human radiation dose estimates.", (1999), Siegel et al.*

*[3] "Evaluation of dosimetry of radioiodine therapy in benign and malignant thyroid disorders by means of iodine124 and PET." European journal of nuclear medicine and molecular imaging, (2002), Eschmann et al.*

*[4] "EANM procedure guidelines for therapy of benign thyroid disease." European journal of nuclear medicine and molecular imaging", (2010), Stokkel, et al.*

*[5] "Radioiodine therapy in benign thyroid disorders. Evaluation of French nuclear medicine practices." Annales d'endocrinologie, (2014), Bernard et al.*

***[6] Melo, Dunstana R., et al. "Organ Dose Estimates for Hyperthyroid Patients Treated with 131I: An Update of the Thyrotoxicosis Follow-Up Study." Radiation research 184.6 (2015): 595-610.***


ICRP Annals of the ICRP

# Image Analysis : Methods

## Raw Image

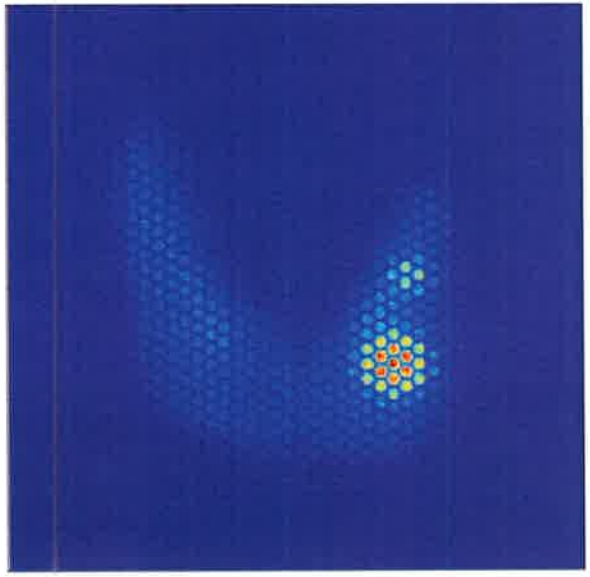

# Image Analysis : Methods

**Raw Image**

**Energy and Spatial gaussian blurring**

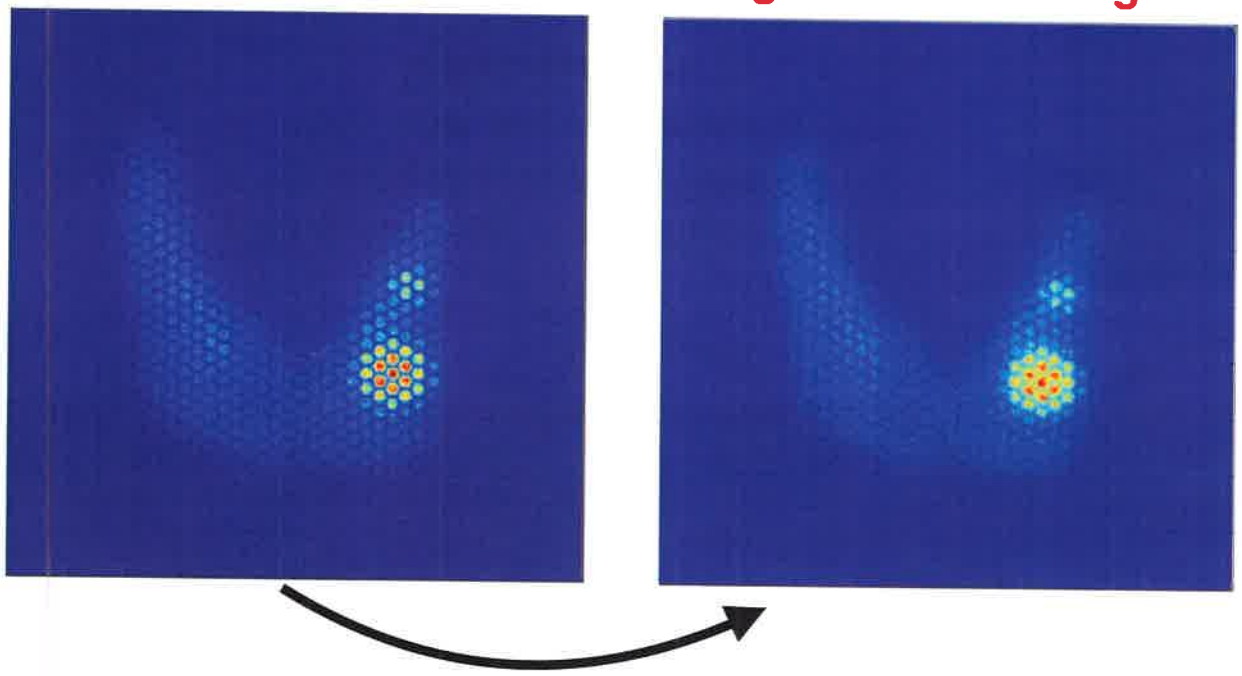

**using Energy Resolution and Spatial Resolution values obtained experimentally**
**$CeBr_3$ 6 mm :**

**SR 1.12 mm @ 122 keV**
**ER 8.1% @ 356 keV**

# Image Analysis : Methods

**Raw Image**

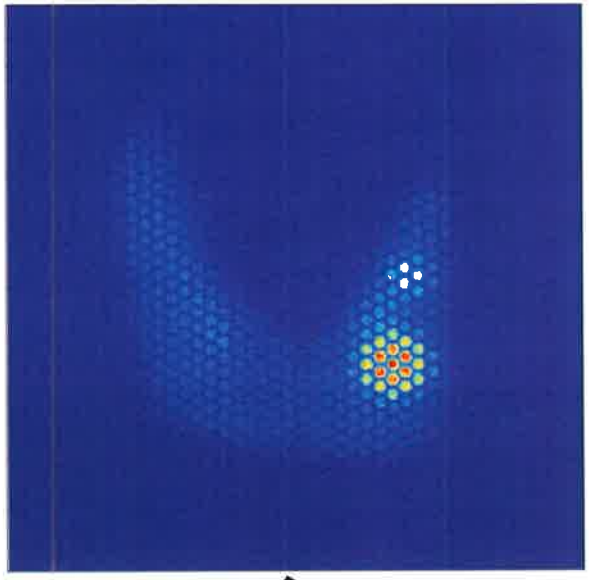

**Energy and Spatial gaussian blurring**

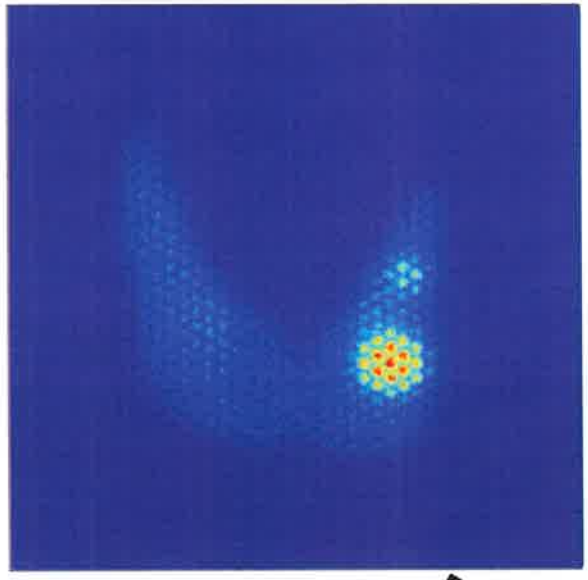

**Frequency filter [7]**

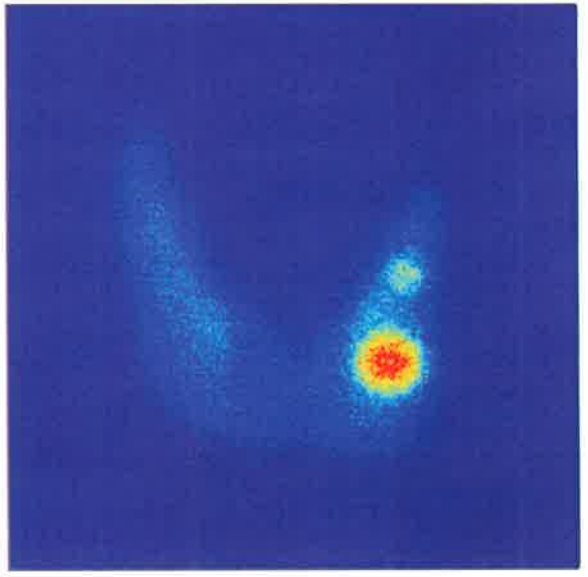

**using Energy Resolution and Spatial Resolution values obtained experimentally $CeBr_3$ 6 mm :**

**SR 1.12 mm @ 122 keV**

**ER 8.1% @ 356 keV**

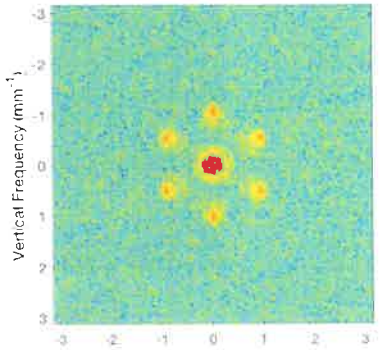


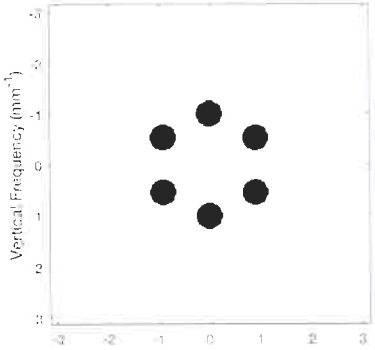


[7] Perez-Garcia, H., and R. Barquero. "The HURRA filter: an easy method to eliminate collimator artifacts in high-energy gamma camera images." (2017)

# Image Analysis : Methods

## Nodule detectability

**Contrast**

$$\frac{Cps_{ROI} - Cps_{BKG}}{Cps_{BKG}}$$

**SNR**
**(Signal-to-noise ratio)**

$$\frac{Cps_{ROI} - Cps_{BKG}}{SD_{BKG}}$$

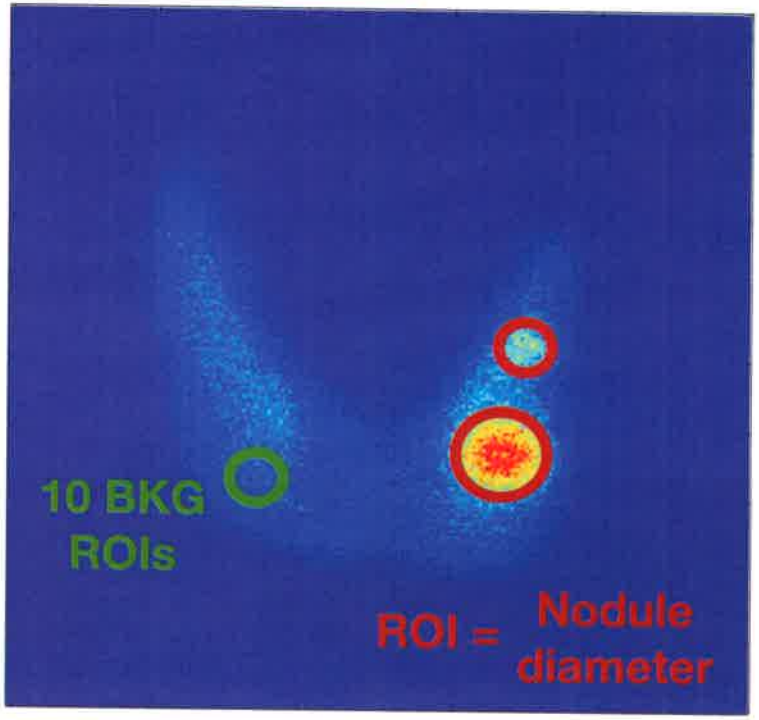

# Image Analysis : Methods

## Nodule detectability

**Contrast**

$$\frac{Cps_{ROI} - Cps_{BKG}}{Cps_{BKG}}$$

**SNR**
**(Signal-to-noise ratio)**

$$\frac{Cps_{ROI} - Cps_{BKG}}{SD_{BKG}}$$

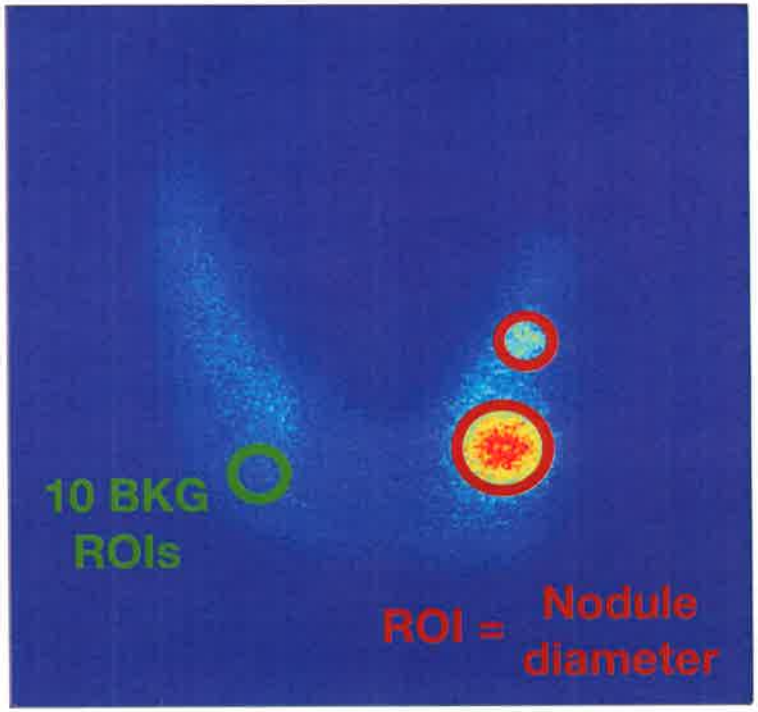


## Activity Quantification

**Recovery Factor**

$$\frac{\text{Estimated Activity}}{\text{Expected Activity}}$$

**Estimated Activity** $= \sqrt{\frac{I_A I_P}{T}} \cdot \frac{f}{C} \cdot k$

*[2] "MIRD pamphlet no. 16: techniques for quantitative radiopharmaceutical biodistribution data acquisition and analysis for use in human radiation dose estimates.", (1999), Siegel et al.*

# Image Analysis : Methods

## Nodule detectability

**Contrast**

$$\frac{Cps_{ROI} - Cps_{BKG}}{Cps_{BKG}}$$

**SNR**
**(Signal-to-noise ratio)**

$$\frac{Cps_{ROI} - Cps_{BKG}}{SD_{BKG}}$$

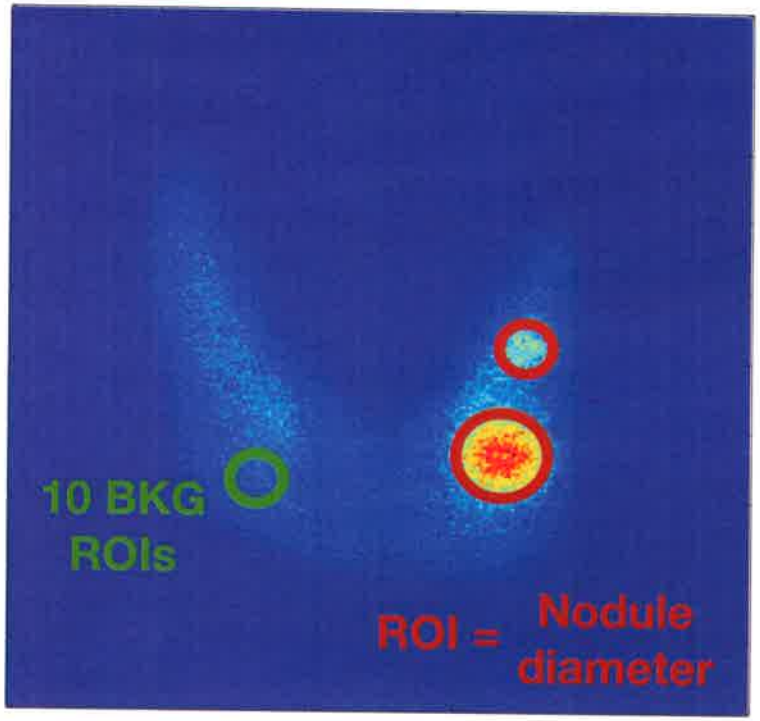


## Activity Quantification

**Recovery Factor**

$$\frac{\text{Estimated Activity}}{\text{Expected Activity}}$$

**Estimated Activity** = $\sqrt{\frac{I_A I_P}{T}} \cdot \frac{f}{C} \cdot k$

$I_A$, $I_P$ Counts/time from the anterior and posterior (A/P) image of the source region ROI

$C$ Calibration factor

$T$ Transmission factor

$k$ Background correction factor

$f$ source self-attenuation correction

*[2] "MIRD pamphlet no. 16: techniques for quantitative radiopharmaceutical biodistribution data acquisition and analysis for use in human radiation dose estimates.", (1999), Siegel et al.*

# Image Analysis : Methods

## Nodule detectability

**Contrast**

$$\frac{Cps_{ROI} - Cps_{BKG}}{Cps_{BKG}}$$

**SNR**
**(Signal-to-noise ratio)**

$$\frac{Cps_{ROI} - Cps_{BKG}}{SD_{BKG}}$$

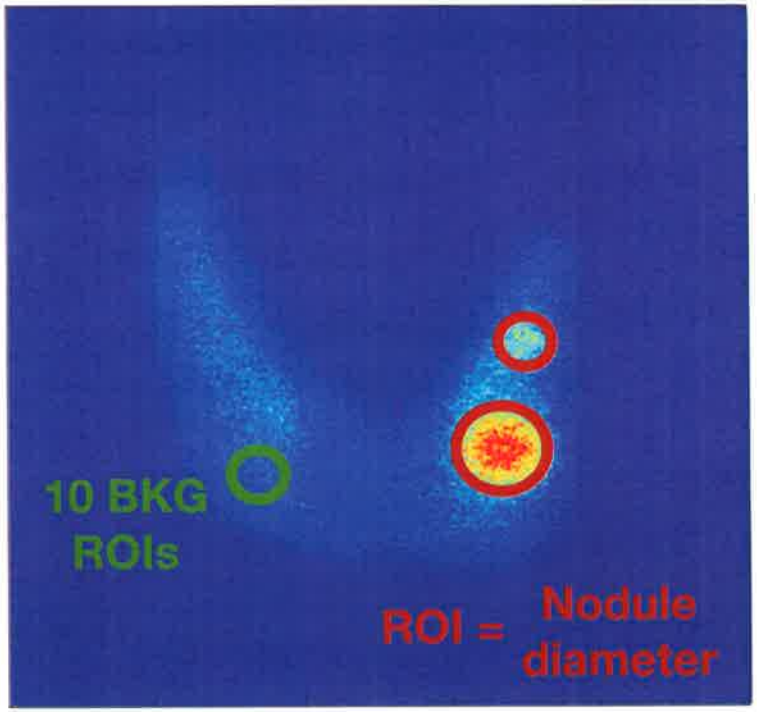


## Activity Quantification

**Recovery Factor**

$$\frac{\text{Estimated Activity}}{\text{Expected Activity}}$$

**Estimated Activity** $= \sqrt{\frac{I_A I_P}{T}} \cdot \frac{f}{C} \cdot k$

$I_A$ Counts/time from the anterior
$I_P$ and posterior (A/P) image of the source region ROI

$C$ Calibration factor — **Simulations**

$T$ Transmission factor — **Estimations**

$k$ Background correction factor

$f$ source self-attenuation correction

*[2] "MIRD pamphlet no. 16: techniques for quantitative radiopharmaceutical biodistribution data acquisition and analysis for use in human radiation dose estimates.", (1999), Siegel et al.*

# Image Analysis : Results

## Contrast

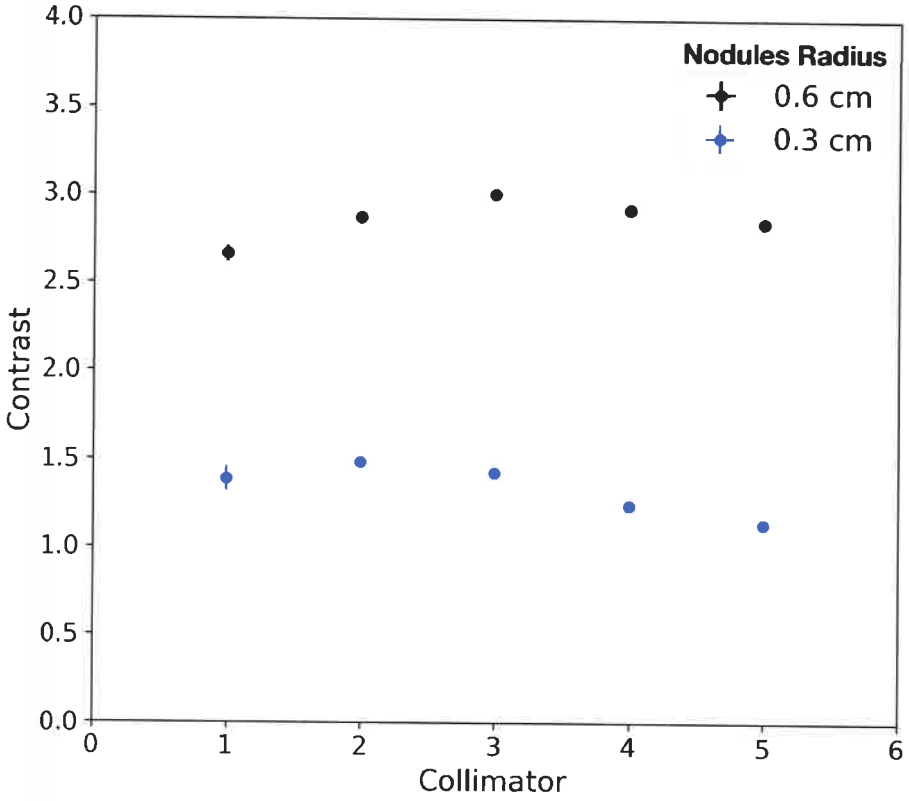


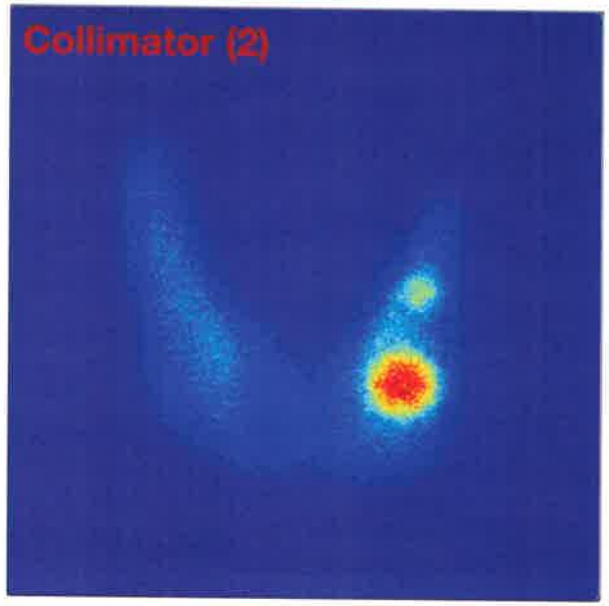


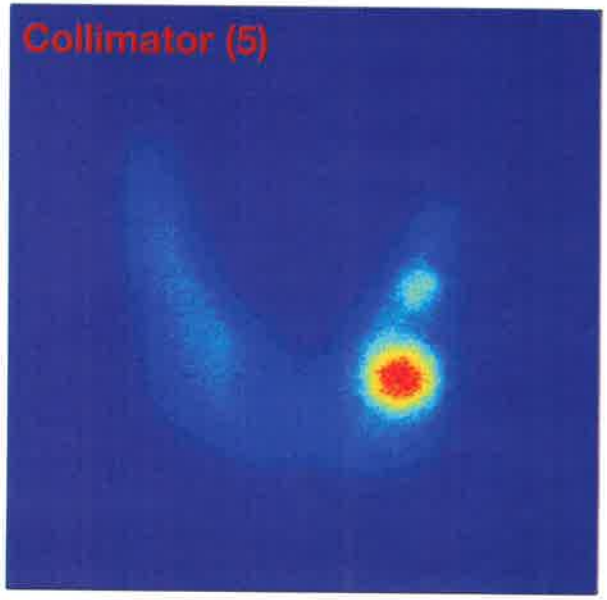


**Higher Partial Volume effect :**

**for lower SR**

**for smaller nodule**

# Image Analysis : Results

**Contrast**

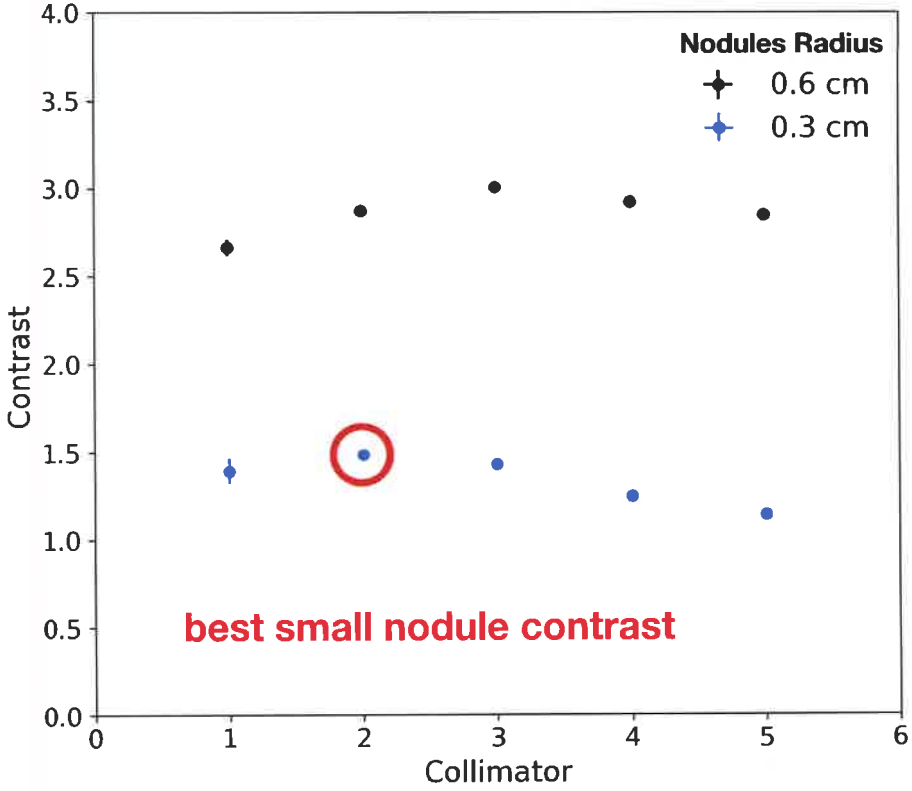


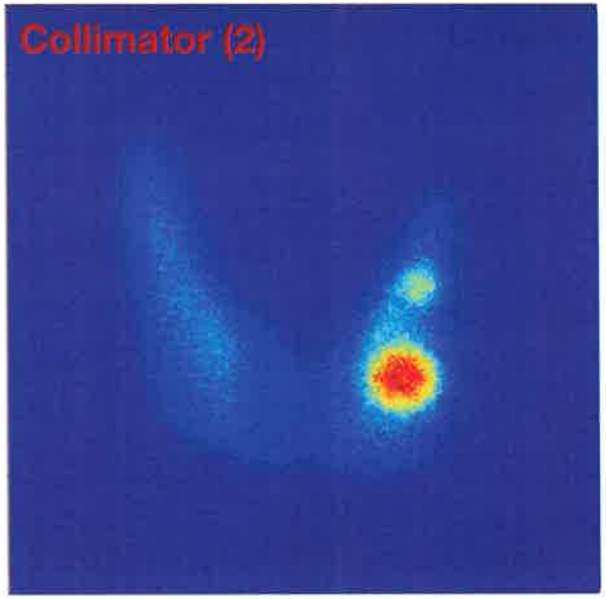


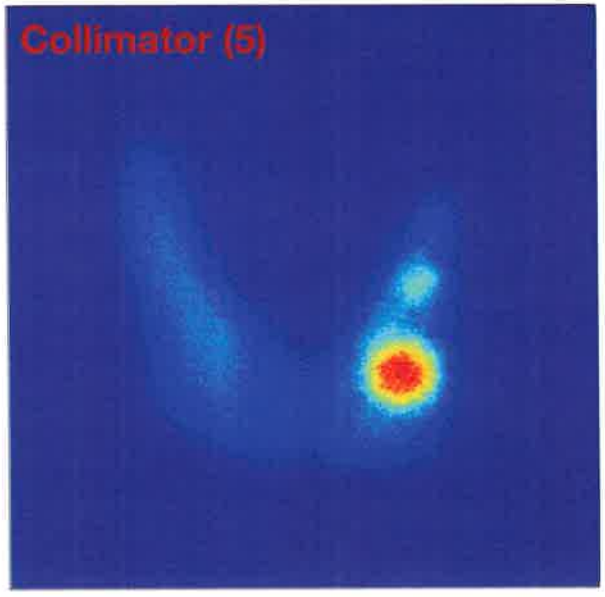


**Higher Partial Volume effect :**

**for lower SR**

**for smaller nodule**

# Image Analysis : Results

**Contrast**

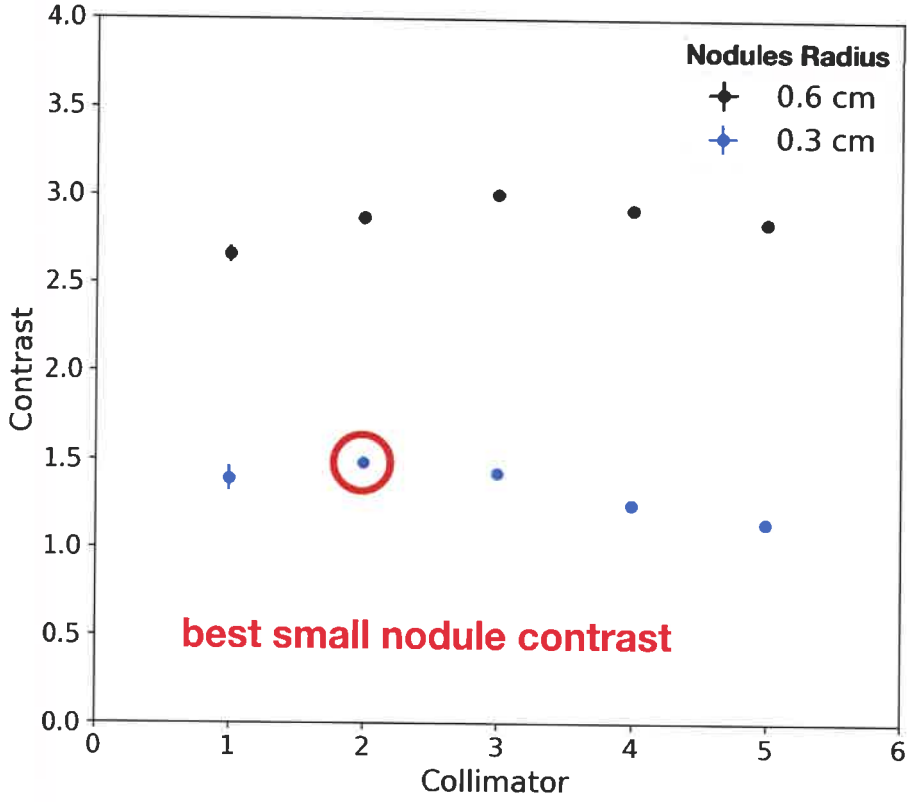


**SNR**
**(Signal-to-noise ratio)**

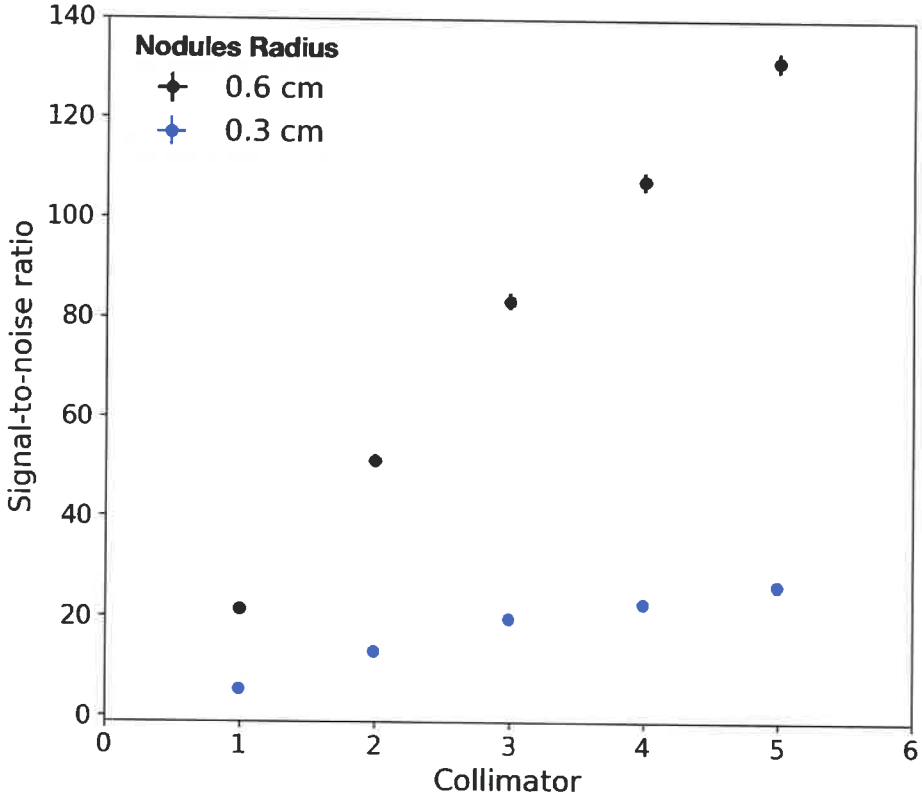


**Higher Partial Volume effect :**

**for lower SR**

**for smaller nodule**

# Image Analysis : Results

## Contrast

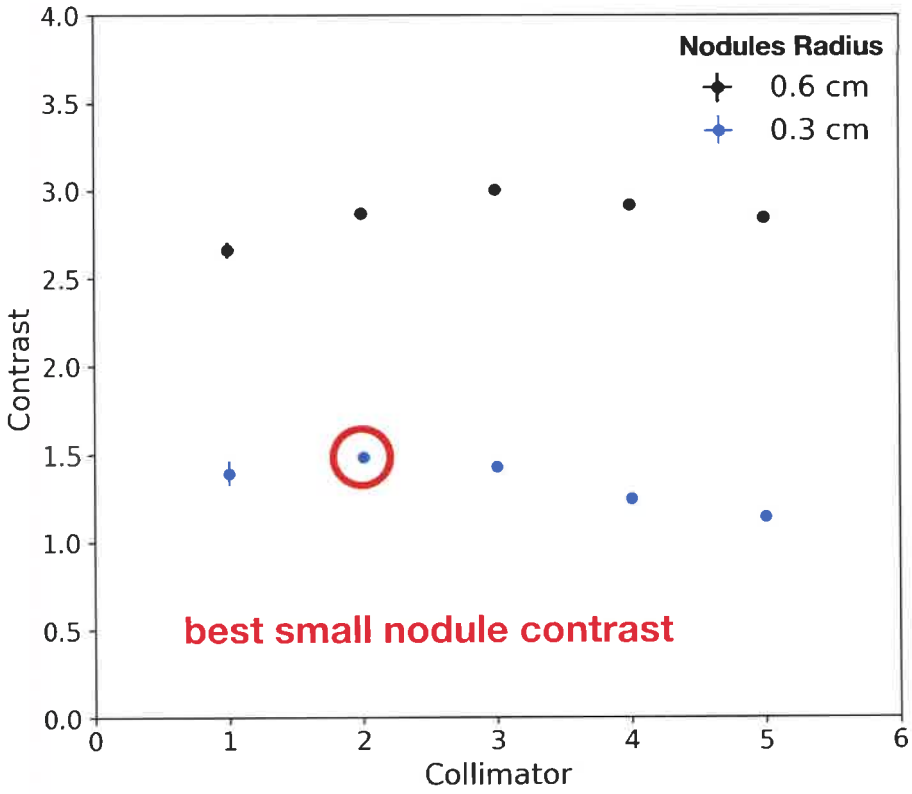


**Higher Partial Volume effect :**

**for lower SR**

**for smaller nodule**

## SNR
**(Signal-to-noise ratio)**

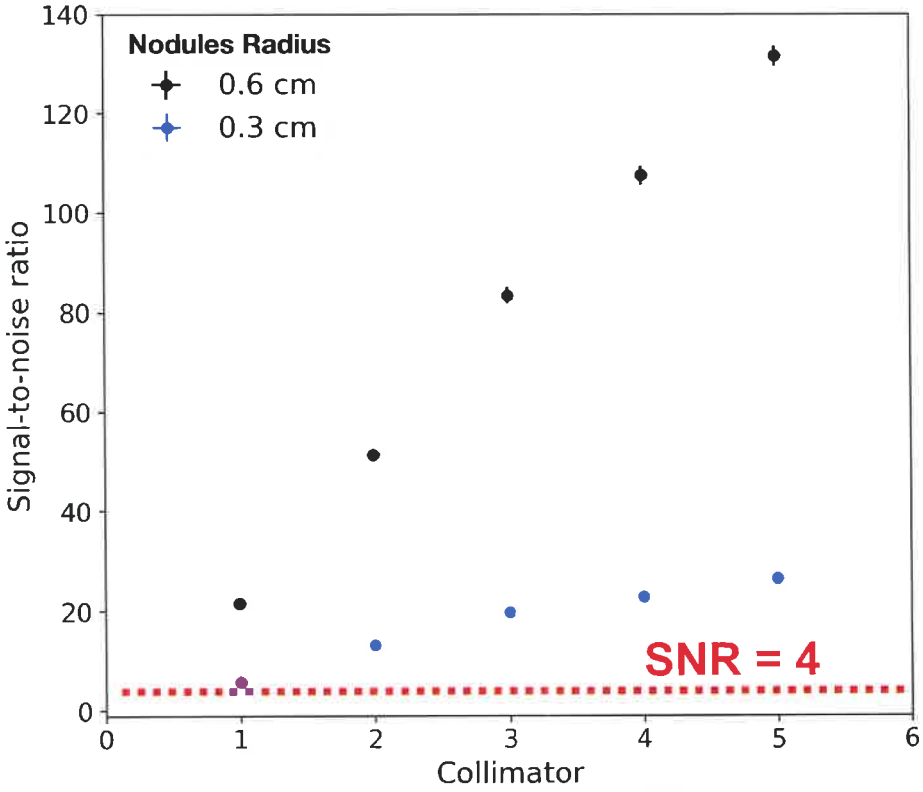


**Detectability with SNR > 4** [8]

**Nodules can be detected with all configurations**

*[8] Waterstram-Rich, et al. Nuclear Medicine and PET/CT-E-Book: Technology and Techniques. Elsevier Health Sciences, 2016.*

# Image Analysis : Results

## Recovery Factor

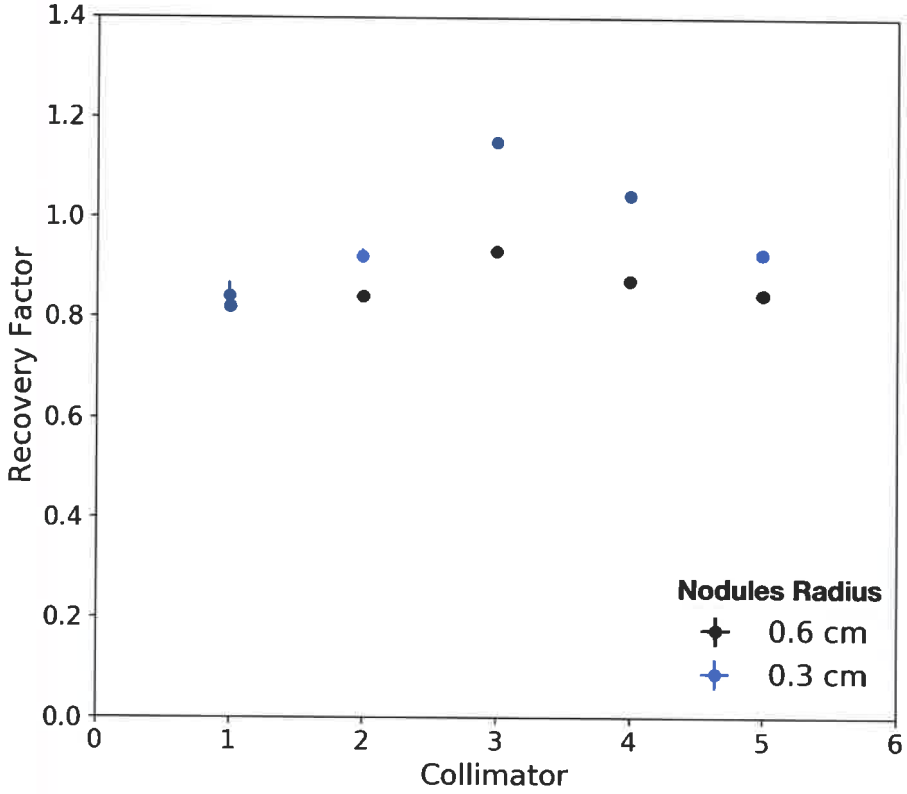


**Obtained with a maximum error of 18 % for all configuration**

**Possible sources of error :**

BKG correction
(harder for small nodule)

Imprecise calibration factor extrapolation

Lack of Diffusion correction

# Image Analysis : Results

## Recovery Factor

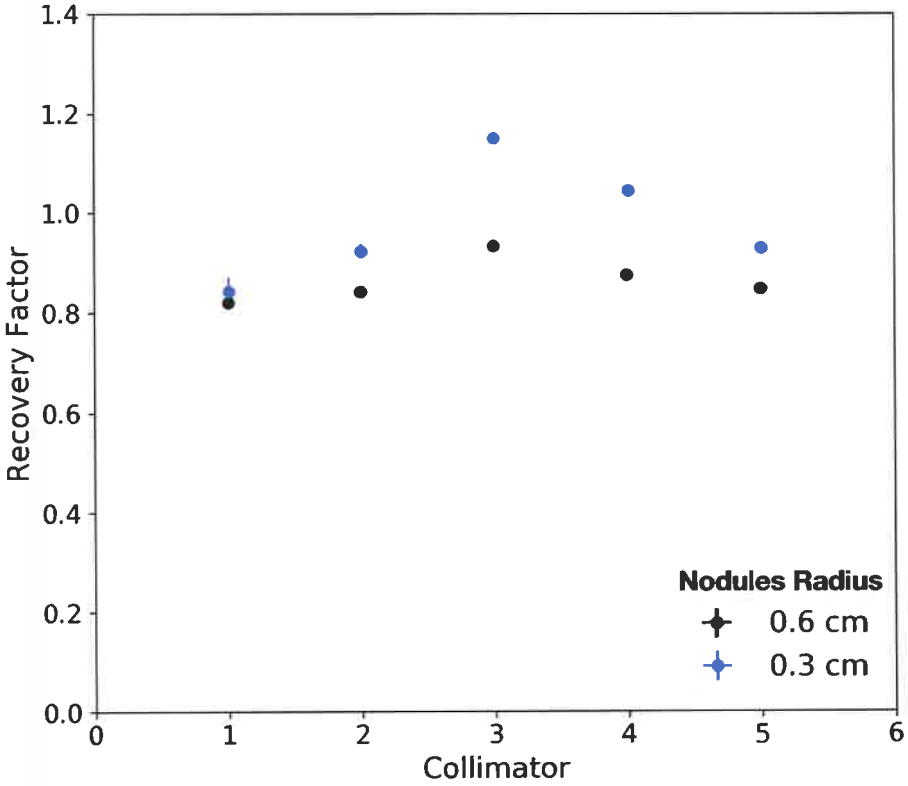


**Obtained with a maximum error of 18 % for all configuration**

**Possible sources of error :**

BKG correction
(harder for small nodule)

Imprecise calibration factor extrapolation

Lack of Diffusion correction

**Best image quality (small nodules) with collimator (2)**

## Collimator 2

| L (cm) | d (cm) | t (cm) | SR (mm) | Efficiency @ 5 cm |
|---|---|---|---|---|
| 5,5 | 0,1 | 0,085 | 2 | $1.24\ 10^{-5}$ |

# Conclusions and Next steps

- **Monte Carlo simulations has been developed to investigate collimator's properties for the detection of high energy gamma in the context of absorbed radiation dose control in targeted radionuclide therapy**

- **The penetration and scatter highly influence image quality and can be estimated only through the use of simulations**

- **Simulations allowed to chose a collimator configurations with good features (SR, E, SP, signal-to-noise ratio) that match our dosimetry goal**

- **Next steps consist in the optimization of quantification protocol : integration of diffusion correction (triple window correction)**

- **Choice of the best scintillator-photodetection assemblies**

- **Integration of a fully operational 5x5 $cm^2$ camera prototype and validation with thyroid phantom**

# Conclusions and Next steps

# Comments

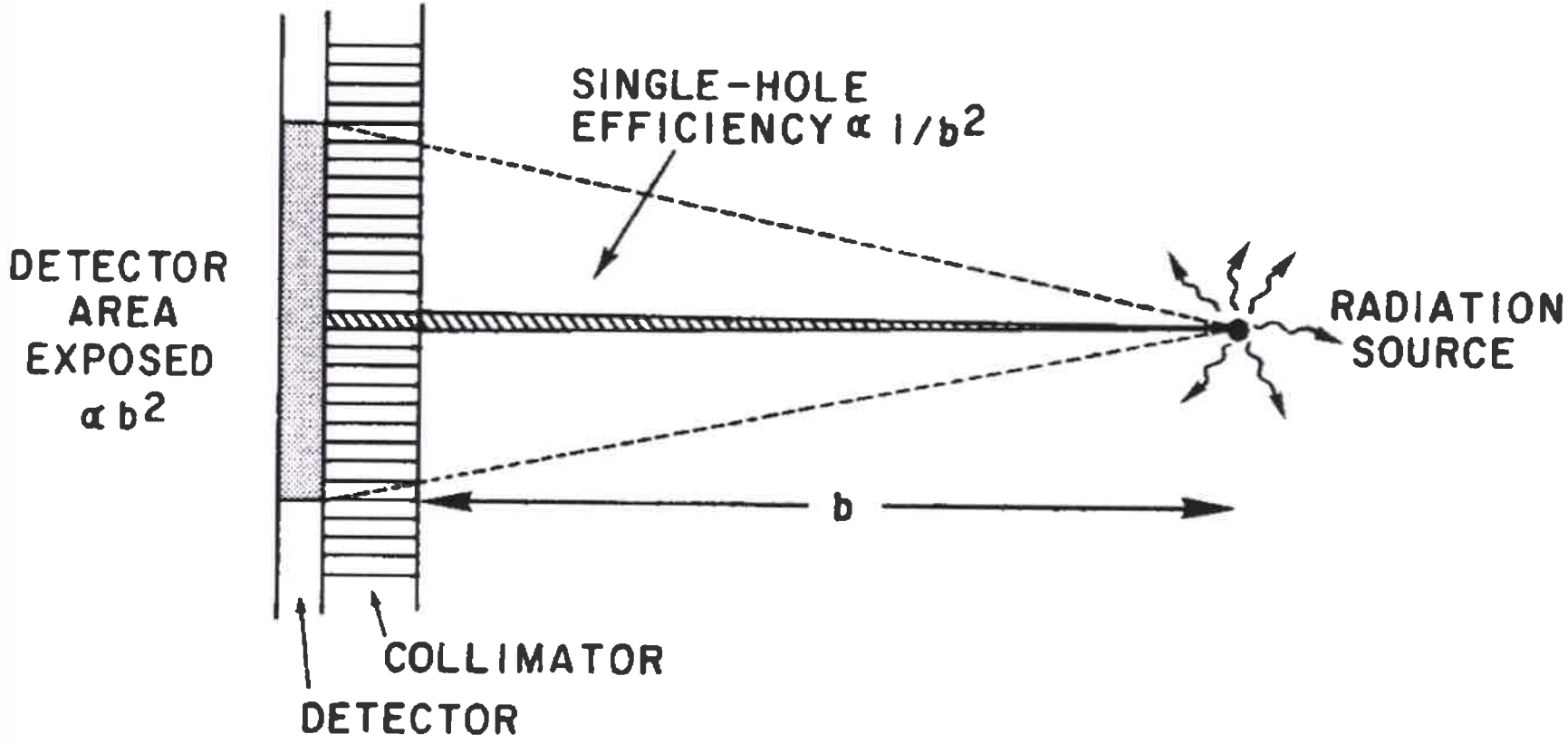
SINGLE-HOLE
EFFICIENCY α 1/b2
DETECTOR
AREA
EXPOSED
α b2
RADIATION
SOURCE
b
COLLIMATOR
DETECTOR

## Background correction

*ii. Analytical Methodology.* Figure 1c illustrates the situation in which a well-defined source is surrounded by background activity uniformly distributed in the adjacent tissue. For this configuration, the source region activity $A_3$ is given by the expression:

$$A_3 = \sqrt{\frac{I_A I_P}{e^{-\mu_c t}}} \frac{f_3}{C} k(\gamma), \qquad \text{Eq. 8}$$

where

$$k(\gamma) \equiv \{1 + (\gamma_2 f_3/f_2)^2 + (\gamma_4 f_3/f_4)^2 + 2\gamma_2\gamma_4(f_3^2/f_2 f_4) \cosh [(\mu_2 t_2 + 2\mu_3 t_3 + \mu_4 t_4)/2] + 2\gamma_2 f_3/f_2 \cosh [(\mu_2 t_2 + \mu_3 t_3)/2] + 2\gamma_4 f_3/f_4 \cosh [(\mu_3 t_3 + \mu_4 t_4)/2]\}^{-1/2}. \qquad \text{Eq. 9}$$

The individual f factors are defined according to Equation 2, whereas $\gamma_2 \equiv A_2/A_3$ and $\gamma_4 \equiv A_4/A_3$ represent the ratios of the activity in the adjacent regions to that in the source volume. Calculation of the $k(\gamma)$ constant requires estimates of the factors ($f_j$, $\gamma_2$, $\gamma_4$) that may be obtained through analysis of additional views in combination with the main conjugate view pair. The $k(\gamma)$ correction may become significant when the activity in the adjacent regions approaches 10% of that in the source volume (*9,16*).

# Comments

where:

$$f_j \equiv \frac{(\mu_j t_j/2)}{\sinh(\mu_j t_j/2)} \qquad \text{Eq. 2}$$

and

$$\mu_e = (1/t)\sum_{i=1}^{n} \mu_i t_i - \mu_j + (1/t)\sum_{i=1}^{n} (\mu_i - \mu_j) t_i. \qquad \text{Eq. 3}$$

# Comments